(17) Ito, T.; Sato, Y.; Yamaguchi, T.; Nakao, S. *Macromolecules* **2004**, *37* (9), 3407–3414.
(18) Kudaibergenov, S. E.; Didukh, A. G.; Zhumadilova, G. T.; Koizhaiganova, R. B.; Bimendina, L. A.; Noh, J. G.; Geckeler, K. E. *Macromol. Symp.* **2004**, *207*, 153–171.
(19) Ende, M. T. A.; Peppas, N. A. *J. Appl. Polym. Sci.* **1996**, *59* (4), 673–685.
(20) Karino, T.; Masui, N.; Hiramatsu, M.; Yamaguchi, J.; Kurita, K.; Naito, S. *Polymer* **2002**, *43* (26), 7467–7475.
(21) Izatt, R. M.; Bradshaw, J. S.; Nielsen, S. A.; Lamb, J. D.; Christensen, J. J. *Chem. Rev.* **1985**, *85* (4), 271–339.
(22) Rotello, V. E. *Nanoparticles Building Blocks for Nanotechnology*; Kluwer Academic/Plenum Publishers: New York, 2004; pp 225–250.

MA801936T

Fabrication of Protein Renaturation Facilitating Membrane Using Plasma Graft Pore Filling Technique

Hidenori Ohashi[†], Maiko Watanabe[†], Taichi Ito[†‡], Takanori Tamaki[†], and Takeo Yamaguchi[†]

[†]Chemical Resources Laboratory, Tokyo Institute of Technology,
R1-17 4259, Nagatsuta-cho, Midori-ku, Yokohama-city, Kanagawa 226-8503, Japan
[‡]Center for Disease Biology and Integrative Medicine Faculty of Medicine, The University of Tokyo
7-3-1, Hongo, Bunkyo-ku, Tokyo 113-0033, Japan

Key words: protein renaturation facilitating membrane, plasma graft polymerization, non-detergent sulfobetaine

1. Introduction

Along with the drastic development of biotechnology, rapid and large scale production of proteins is highly demanding for pharmaceutical usage including antibody drug, identification of biological function of recombinant, key constituent of biodevices, and so on. Protein expression in Escherichia coli (E. coli) is most convenient and frequently used method due to its capability of high-level expression and versatility for most proteins including protease. In the expression within E. coli, protein is usually yielded in the form of inclusion body, which is insoluble, inactive aggregate. In order to recover biological activity of resultant protein, solubilization and renaturation processes are inevitably required, and the latter to reconstruct protein three dimensional exact structure is most problematic in most cases.

To increase renaturation efficiency and to reduce expensive reagent in the renaturation process, handlings of dilution, dialysis, chromatography, and solid phase have been investigated [1,2]. At the same time, a number of additive helper agents to enhance protein folding has been extensively explored. However, most of the previously-proposed methods are batch process and only very few study including continuous fed batch system [3] can be found as continuous renaturation process. Development of versatile continuous renaturation approach can offer opportunity for further mass production and facile approach to useful protein.

Although it has never been thoroughly explored, membrane process is one of the candidates of such promising continuous renaturation operation due to lower energetic expense and higher throughput capability, if proper membrane that can facilitate protein folding within itself can be fabricated. In order to fulfill the requirement, a renaturation helper agent should be immobilized on the membrane in a controlled way. The membrane will be also feasible as a key unit of persistent bioreactor that retains protein functionality by continuously refolding deactivated protein.

Non-detergent sulfobetaine (NDSB) is one of the candidates that have been proven to work as the folding facilitating helper for several proteins [4,5]. NDSB is a zwitterion having both of positive and negative charges, hydrophobic groups within the molecule, and was shown to prevent protein aggregation by stabilizing protein molten globule state: early folding intermediate [6]. As schematically shown in Figure 1, immobilization of such NDSBs in the form of linear polymer for fully retaining mobility of the helper and accessibility to protein is favorable as renaturation facilitating membrane. In the present study, NDSB having vinyl group was first synthesized, and then, was immobilized onto pore surface of porous substrate using plasma graft polymerization technique in order to envision the idea.

2. Experimental

2.1.Materials

Porous polyethylene (PE) film was used as the porous substrate. The PE substrate with a thickness of 90 μm, a pore diameter of 200 nm, and porosity of 50% was kindly supplied by Asahi Chemical Co. Ltd., Japan. *N*-(3-dimethyl aminopropyl) methacryl amide (DMAPMA) was purchased from TCI, Tokyo, Japan, and 1,3-propanesultone was purchased from Aldrich Japan, Tokyo, Japan. All of other materials were purchased from Wako Pure Chemicals, Osaka, Japan, and were used without

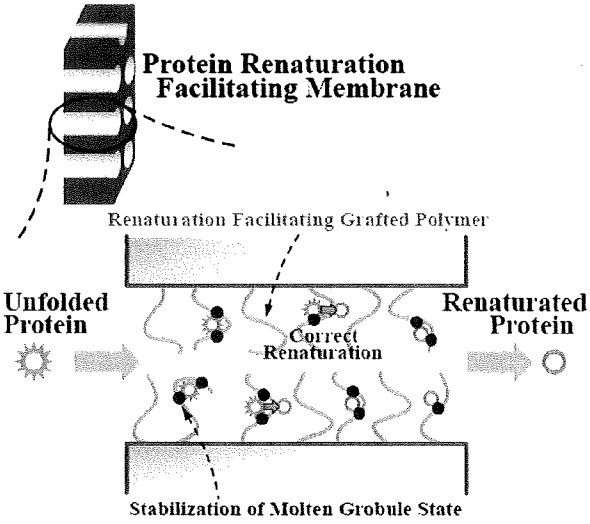

Figure 1. Schematic illustration of protein renaturation facilitating membrane: immobilized renaturation facilitating linear polymer help unfolded protein to recover folded structure.

any further purification if not otherwise noted.

2.2. Synthesis of NDSB monomer, *N,N*-dimethyl (methacrylamidopropyl) ammonium propanesulfonate (DMMAAPS)

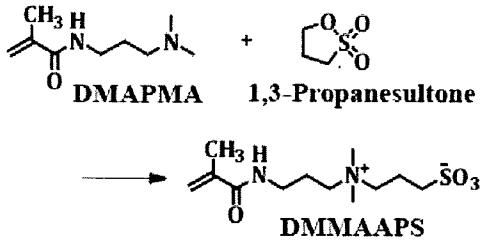

Scheme 1. Synthesis scheme of non-detergent sulfobetaine monomer, *N,N*-dimethyl (methacrylamidopropyl) ammonium propanesulfonate (DMMAAPS).

DMMAAPS, non-detergent sulfobetaine having vinyl group, was synthesized along with Scheme 1 based on the previous study [7]. *N*-(3-dimethyl aminopropyl) methacrylamide (DMAPMA) was purified by distillation under reduced pressure. 1,3-Propanesultone (3.66 g) dissolved in acetonitrile (3 g) was added dropwise into above-distilled DMAPMA (5.11 g) and hydroquinone (0.06 g) in acetonitrile (10 g) at 70 °C with agitation. The solution was stirred at 70 °C for 7 hours, then at 30 °C for 48 hours. Filtered solid of the solution was washed with acetone several times, and was vacuum dried for 12 hours. The resultant solid was 8.33 g (yield was 95.0%) and successful synthesis of DMMAAPS was confirmed by ^{1}H-NMR.

2.3. Preparation of NDSB immobilized membrane using plasma graft polymerization

Acrylamide (AAm) was purified by recrystalization from ethyl acetate. An aqueous solution of DMMAAPS and AAm emulsified with sodium dodecyl sulfate (SDS) was used as monomer solution for plasma graft polymerization. Both the total monomer concentration and SDS in solution were fixed at 5.0 and 5.0 wt%, respectively. The mole fraction of DMMAAPS in the monomers was 100 or 10 mol%. Porous PE substrate was treated with an argon plasma with the pressure of 10 Pa and then was exposed to air for 60 s to generate peroxide groups on its pore surface [8,9]. The substrate containing peroxide groups was immersed into extensively degassed (freeze-thawed) monomer solution. By holding the solution at 80 °C, the peroxide groups were broken to give active radical sites, and graft polymerization reaction started from the initiator radicals. Reaction time was set at 1 hour. Resulting membrane was extensively washed with water and ethanol several times, and analyzed by weight increase and FT-IR after drying.

3. Results and Discussion

Filling ratio of the fabricated membrane is defined as following equation.

$$\text{Filling ratio} = \frac{\text{Volume of grafted polymer}}{\text{Pore volume of porous substrate}}$$

Density of vinyl polymer does not vary so much, thus in the present study, it is regarded as 1.0 [10]. In porous PE substrate, outer surface area is negligible compared with surface area of pore surface, thus contribution of outer surface area was ignored. When DMMAAPS was used as the sole monomer, filling ratio after one hour reaction was as low as 1.6%, although the immobilization of sulfonyl group of DMMAAPS was confirmed by FT-IR around 1050 and 1200 cm^{-1} shown in Figure 2(b). Even one week reaction yielded 2.5% filling ratio and the ratio was not improved by the elongated reaction time. This should be due to the low reactivity of the NDSB monomer for the plasma graft polymerization. In order to enhance the grafting amount, AAm was graft-copolymerized with the NDSB monomer; AAm can also increase hydrophilicity of the graft polymer, which works advantageous for prevention of non-specific protein adsorption. One hour reaction using 10 mol% DMMAAPS and 90 mol% AAm as monomer mixture improved filling ratio towards 7.2%, which is less than 9% having small quantity of long graft chain inside the membrane prepared by the same technique [11]. This means pores of the fabricated membrane are possibly in open state and it is the aimed structure indicated in Figure 1. Furthermore, in the case of plasma graft polymerization, chain density was calculated to be about 0.01 nm^{-2}, which is in semidilute region [11]: it allows protein to access inside the linear polymer brush with the renaturation assistant moiety. FT-IR characterized as Figure 2(c) confirms successful immobilization of DMMAAPS and AAm characterized by above-observed sulfonyl peaks and stronger peak of amide I around 1650 cm^{-1}.

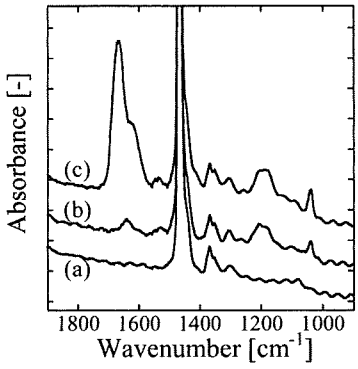

Figure 2. IR spectra of (a) porous PE substrate, (b) polyDMMAAPS grafted membrane (1.6%), and (c) poly(DMMAAPS-*co*-AAm) grafted membrane (7.2%).

In the literature, optimal concentration for renaturation of various NDSBs was reported to be 0.4 to 2.0 mol/L [4], which amounts to as high as 0.1 to 0.4 g/ml. NDSB content of the membrane fabricated in the present study can be calculated to be 0.02 to 0.03 g/ml and this value might not be sufficient for the membrane facilitated protein renaturation. In order to attain higher NDSB content in the membrane, longer reaction time, optimal ratio between NDSB monomer and hydrophilic comonomer, development of easy polymerizable monomer, would be required. Alternatively, an optimal NDSB content of membrane may be different from that of small molecular helper due to immobilization and/or cooperative effect. In order to investigate the potential effects and the performance of the fabricated membrane, renaturation experiment using permeation apparatus must be executed and the trial is now under way.

4. Conclusion

For the fabrication of protein renaturation facilitating membrane, DMMAAPS, one of the non-detergent sulfobetaines, which function as an effective renaturation assistance, was immobilized onto porous PE substrate for the first time, via using plasma graft polymerization technique. DMMAAPS alone was found to be difficult to immobilize using the technique probably due to its low reactivity, however plasma graft copolymerization of DMMAAPS with AAm can adequately enhance the filling ratio to 7.2%, whose pores can be in open state accessible by proteins. Further investigation on the performance of the membrane will open the probability of continuous protein renaturation process, which is promising for facile protein production.

References

1. E. B. Clark, *Cur. Opinion Biotech.*, **12** (2001) 202.
2. K. Tsumoto, D. Ejima, I. Kumagai and T. Arakawa, *Protein Express. Purif.*, **28** (2003) 1.
3. S. Katoh and Y. Katoh, *Proc. Biochm.*, **35** (2000) 1119.
4. N. Expert-Bezancon, T. Rabilloud, L. Vuillard and M. E. Goldberg, *Biophys. Chem.*, **100** (2003) 469.
5. S. D'Amico and G. Feller, *Anal. Biochem.*, **385** (2009) 389.
6. L. Vuillard, T. Rabilloud, and M. E. Goldberg, *Eur. J. Biochem.*, **256** (1998) 128.
7. W. F. Lee and Y. M. Chen, *J. Appl. Polym. Sci.*, **91** (2004) 726.
8. T. Yamaguchi, S.-I. Nakao, and S. Kimura, *Macromolecules*, **24** (1991) 5522.
9. M. Suzuki, A. Kishida, H. Iwata, and Y. Ikada, *Macromolecules*, **19** (1986) 1804.
10. N. Miyaoi, H. Ohashi, T. Ito and T. Yamaguchi, *J. Chem. Eng. Japan*, **41** (2008) 766.
11. H. Kuroki, H. Ohashi, T Ito, T Tamaki and T. Yamaguchi, *J. Membr. Sci.*, **352** (2010) 22.

Journal of Membrane Science 352 (2010) 22–31

Contents lists available at ScienceDirect

Journal of Membrane Science

journal homepage: www.elsevier.com/locate/memsci

Isolation and analysis of a grafted polymer onto a straight cylindrical pore in a thermal-responsive gating membrane and elucidation of its permeation behavior

Hidenori Kuroki[a], Hidenori Ohashi[b], Taichi Ito[b,c], Takanori Tamaki[b], Takeo Yamaguchi[a,b,*]

[a] Chemical System Engineering, The University of Tokyo, Japan
[b] Chemical Resources Laboratory, Tokyo Institute of Technology, Japan
[c] Center for Disease Biology and Integrative Medicine, The University of Tokyo, Japan

ARTICLE INFO

Article history:
Received 29 October 2009
Received in revised form 20 January 2010
Accepted 23 January 2010
Available online 1 February 2010

Keywords:
Graft polymerization
Gating membrane
Thermal-responsive polymer
Permeability

ABSTRACT

We have attained the thermal-responsive gating membrane with a drastic permeability change by several hundredfold; *N*-isopropylacrylamide (NIPAM) polymers were grafted on the pore surface by the plasma-induced graft polymerization. In this study, we fabricated the gating membrane using a polycarbonate (PC) substrate with straight cylindrical pores. This substrate can be degraded in a strong-alkaline solution, thus the grafted NIPAM polymer was isolated from the substrate and evaluated. Accordingly, we found the grafted polymer has a high molecular weight (from several hundred thousand to a few million) and the polymer chain density is low at *ca.* 0.01 chains nm^{-2}. These results indicate factors significant to drastic pore gating; the pores are fully open in a shrunken state at the low chain density, by the existence of enough space for shrinking grafted polymers. Further, the pores are sufficiently closed by swollen NIPAM polymers with a small number of high molecular weight polymers. From the above, we clarified the relationship between the property of the grafted polymer and the permeation behavior of the thermal-responsive gating membrane for the first time. Moreover, the knowledge obtained in this study can provide useful guideline for clarifying the gating function obtained by other grafting technique.

1. Introduction

Stimuli-responsive gating membranes have received much attention in recent years owing to their unique function. They have a functional gate that is responsive to environmental and molecular signals, such as temperature [1–10], pH [11–15], light [16], reduction–oxidation state [17], glucose concentration [18,19], and specific ions [20–22]. Many gating membranes are fabricated by grafting stimuli-responsive polymers onto the porous substrate, as shown in Fig. 1. The swelling–shrinking change in stimuli-responsive grafted polymers on the pore occurs in response to environmental stimuli; thus, pore gating (open/closed) can be controlled. The drastic change in the pore size in response to an environmental signal is a necessary function for the gating membrane. That is, the pores are open in the shrunken state of the grafted polymer—nearly equal to the pore size of the nongrafted porous substrate—and are fully closed in the swollen state of the grafted polymer. The potential applications of these gating membranes, which are responsive to various signals, include flow control, size-selective filtration, chemical and bioseparation, controlled release of chemical substances and drugs, and chemical and biosensors.

To graft a stimuli-responsive polymer onto a porous substrate, radiation-, photo-, and plasma-induced graft polymerization techniques are employed [1–6,13–17,19–24]. Recently, a grafting technique using atom transfer radical polymerization has also been developed [9,10,25]. Among these techniques, plasma-induced graft polymerization has characteristics as described below [23,26–32]. The vacuum ultraviolet rays contained in the plasma play an important role in plasma-induced graft polymerization; they mainly provide radicals on the pore surface without the degradation of a substrate matrix, resulting in the surface grafting. Moreover, radicals are formed inside a porous substrate by plasma treatment, and the grafted polymer is immobilized on the pore surface inside a substrate. Therefore, several studies reported gating membranes using plasma-induced graft polymerization and membrane performances such as permeation flux or solute diffusivity. The stimuli-responsive gating membrane fabricated by plasma-induced graft polymerization successfully exhibited a drastic change in permeation flux in response to an environmental

* Corresponding author at: 4259 Midori-ku, Yokohama, Kanagawa 226-8503, Japan. Tel.: +81 45 924 5254; fax: +81 45 924 5253.
E-mail address: yamag@res.titech.ac.jp (T. Yamaguchi).

0376-7388/$ – see front matter © 2010 Elsevier B.V. All rights reserved.
doi:10.1016/j.memsci.2010.01.052

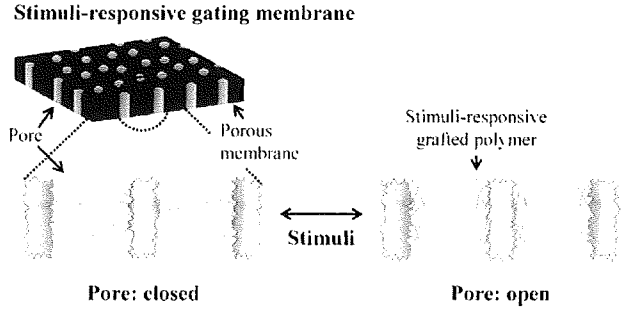

Fig. 1. Schematic illustration of a stimuli-responsive gating membrane caused by grafting a stimuli-responsive polymer onto the pore surface of a porous membrane.

signal. However, there has been no research discussing the relationship between the properties of a grafted polymer and the pore gating in the gating membrane; thus, the underlying mechanism of the abovementioned gate function is unknown. This is because it is difficult to evaluate the properties of a grafted polymer, which is chemically immobilized on a substrate, and thus, little has been reported about the properties of a grafted polymer in a grafted membrane.

In this study, we clarify the relationship between the properties of a grafted polymer in the membrane pore and the permeation behavior of a thermal-responsive gating membrane. Here, we fabricate the thermal-responsive gating membrane using plasma-induced graft polymerization. Poly(*N*-isopropylacrylamide) (NIPAM) is used as the thermal-responsive polymer [33], and a polycarbonate track-etched membrane with straight cylindrical pores is used as the porous substrate. Straight cylindrical pore is suitable for evaluating the permeation behavior. Moreover, a grafted polymer chemically immobilized on the pore surface can be evaluated using a polycarbonate porous membrane. A few previous studies have reported that the grafted polymer was isolated from a substrate by degrading only the substrate composed of cellulose acetate or silica glass [34,35]. Similarly, only the polycarbonate membrane can be degraded by the hydrolysis of the polycarbonate ester bond; thus, the grafted polymer on the pore surface is isolated from the porous substrate and the properties of the grafted polymer are evaluated. Finally, based on the obtained results, we discuss the relationship between the properties of the grafted polymer and the permeation behavior of a thermal-responsive gating membrane for the first time. The clarification of the microscopic phenomena in the membrane pore will prove helpful in designing gating functions.

2. Experimental

2.1. Materials

Cyclopore®, a polycarbonate (PC) track-etched membrane having straight cylindrical pores and uniform pore size and distribution (pore size 0.2 μm, thickness 11 μm, porosity 17%), was purchased from the SPI Supplies Division of Structure Probe, Inc., and used as the porous substrate. NIPAM was supplied by Kohjin Co., Ltd., and was used after purification by recrystallization in hexane and acetone. All other reagents and solvents were purchased from Wako Pure Chemical Industries, Ltd., and used without further purification.

2.2. Fabrication of the thermal-responsive gating membrane

Thermal-responsive gating membranes (PC(NIPAM) membranes) were fabricated by grafting poly(NIPAM) onto the pore surface of the PC porous substrate by plasma-induced graft polymerization, as reported in our previous studies [20,27]. A schematic of plasma-induced graft polymerization is shown in Scheme 1. First, the PC substrate was treated with argon plasma at a pressure of 10 Pa. During plasma treatment, the substrate was placed in a glass ampoule. The plasma treatment power and time were 30 W and 1 min, respectively. The treated membrane was exposed to air for 60 s to generate a peroxide group on its pore surface. Then, the substrate containing the peroxide group was immersed in an extensively degassed (frozen and thawed) aqueous solution of 5 wt% NIPAM monomer, with SDBS as a surfactant. The active radical sites on its pore surface were formed by thermal cleavage of the peroxide group in the solution at 80 °C, and a graft polymerization reaction started from the initiator radical. The reaction time was varied from 20 to 90 min to control the filling ratio. After the polymerization, any remaining monomers and surfactants were removed by rinsing the membrane with a 50% aqueous ethanol solution and hexane. The fabricated PC(NIPAM) membranes were evaluated by weight change, FT–IR (FT/IR 6200; JASCO, Japan), and SEM (S-5200, Hitachi, Japan). By calculating the properties of this PC substrate, the area ratio of the inner surface (the pore surface) and the outer surface is 96% and 4%, respectively. With the assumption of the homogeneous grafting on the membrane surface (the inner and outer surface) by our previous study [30], the outer surface is very small, thus we consider the pore surface as the membrane surface in this study. The filling ratio ϕ of PC(NIPAM) membrane is defined as

$$\phi[\%] = \frac{W_{dry} - W_{sub}}{\rho_{polym} \cdot V_{pore}} \times 100 \quad (1)$$

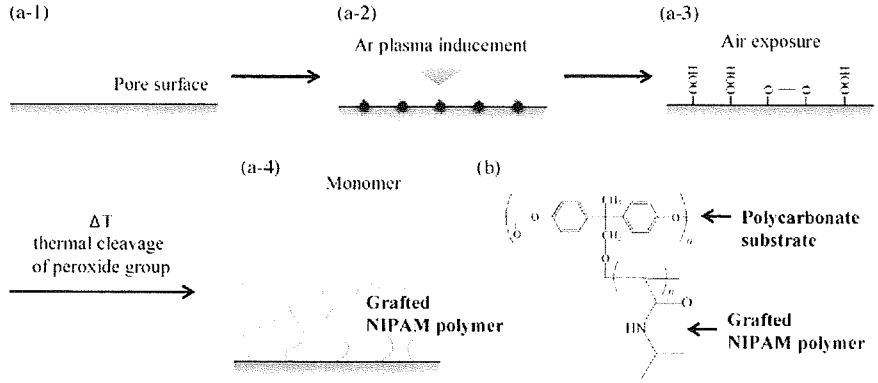

Scheme 1. Scheme of peroxide plasma graft polymerization: (a-1) pore surface of polycarbonate substrate before plasma graft polymerization; (a-2) radical activation induced by Ar plasma; (a-3) formation of peroxide group on exposure to air; (a-4) polymer propagation in monomer solution; and (b) chemical structure of grafted NIPAM polymer on polycarbonate substrate.

where W_{dry} (g) and W_{sub} (g) represent the dry weight of the PC(NIPAM) membrane and the PC substrate, respectively. ρ_{polym} (g/cm^3) is the density of the NIPAM polymer, and is assumed to be 1.0 g/cm^3. V_{pore} (cm^3) is the pore volume of the substrate.

Using the same method, plasma-induced graft polymerization of five sheets of the porous PC substrate was performed. Five sheets of the PC substrate were laid on top of each other, and the edges of the substrates were bound together by heat. The substrate composed of five sheets of the PC substrate is called sandwiched PC substrate hereafter. After the polymerization, the five porous membranes were peeled apart and each sheet was washed by a 50% aqueous ethanol solution and hexane. The sheets were numbered from one to five. The first sheet was closest to the plasma and the fifth sheet rested against the glass wall. The amount of grafted polymer in each sheet was estimated by FT-IR analysis. The peak ratio of P1 (Amide I at 1650 cm^{-1} derived from NIPAM) per P2 (Carbonyl stretching vibration at 1770 cm^{-1} derived from the PC substrate) adopted the maximum value in each sheet, which was suitable for discussing plasma-induced graft polymerization.

2.3. Measurement of water permeability through the thermal-responsive gating membrane

Water permeation flux through the fabricated PC(NIPAM) membrane was measured using the filtration apparatus described in a previous paper [20]. Pure water was passed through a feed chamber and an appropriate pressure (0.2–1.0 kg f/cm^2) was applied across the membrane. The permeability coefficient was calculated from the amount of permeated water. Here, to eliminate the effect of the applied pressure and media viscosity on the permeation flux J [m^3/(s cm^{-2})], the permeability coefficient L_p [m(kg f s cm^{-2})$^{-1}$] was used to evaluate the membrane permeability. L_p is defined in Eq. (2):

$$L_p = \frac{J}{\Delta P \cdot (\mu_{20\,^\circ C}/\mu_T)} \quad (2)$$

where ΔP (kg f/m^2) is the pressure applied across the membrane, and $\mu_{20\,^\circ C}$ (Pa s) and μ_T (Pa s) represent the media viscosity at 20 °C and the measurement temperature, respectively. In this series of measurements, the measurement temperature was varied from 20 to 50 °C, and the filling ratio was varied from 0 to 65%.

2.4. Isolation and analysis of a grafted NIPAM polymer on a polycarbonate substrate

The grafted NIPAM polymer chemically immobilized on the pore surface was isolated from the PC porous substrate by the protocol shown in Scheme 2. The fabricated PC(NIPAM) membrane was immersed in 5 M NaOH aqueous solution and then the mixture was shaken at 80 °C for 3 days. The ester bond of polycarbonate was hydrolyzed in a strong-alkaline, high-temperature solution; thus, only a PC substrate was degraded. After the degradation of the PC substrate and cooling to room temperature, the grafted NIPAM polymer was precipitated in a 5 M NaOH aqueous solution by salting-out, and then the grafted NIPAM polymer was obtained by filtering and washing in 5 M NaCl aqueous solution. Subsequently, the filtered solution was neutralized by HCl and then evaporated. The obtained white solid was washed in acetone and removed by filtering. Then, the filtered solution was evaporated and the PC substrate residue was obtained. The obtained grafted NIPAM polymer and PC substrate residue were analyzed by ^{1}H NMR (Lambda-300; JEOL, Japan) analysis and gel permeation chromatography (GPC, L-7100 Hitachi Ltd., Shodex Oven A0-30 Showa Denko K.K., Shodex RI-71 Showa Denko K.K., Shodex Asahipak GF-7M HQ and KD-806M columns Showa Denko K.K.) measurement. Dimethylformamide solution containing 0.03 M LiBr was used as the eluent

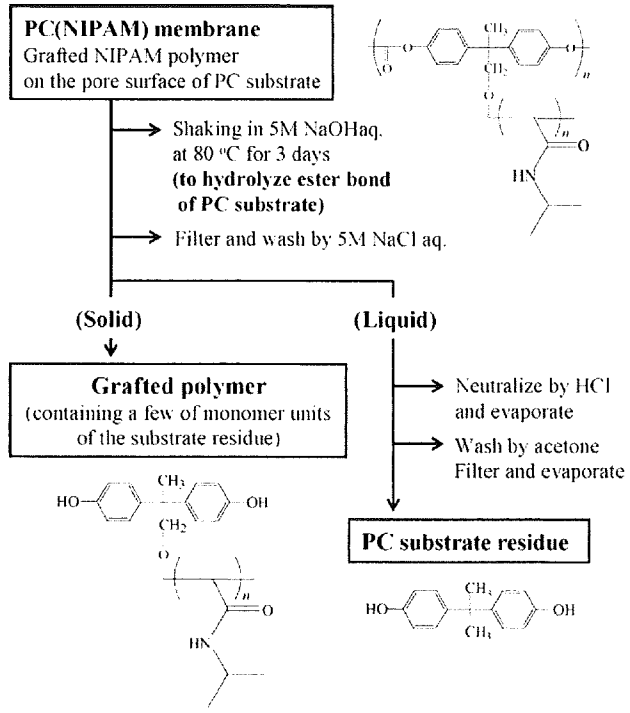

Scheme 2. Scheme to isolate the grafted NIPAM polymer from the PC(NIPAM) membrane.

at a flow rate of 0.5 mL/min. A standard curve was made using a polystyrene standard solution (TSK, Tosoh Corp.). The weight and the number average molecular weight (Mw and Mn) were calculated by the standard curve. The chain density σ (chains/nm^2) of the grafted polymer on the pore surface is defined by Eq. (3):

$$\sigma = \frac{\sum N_i}{S_{pore}} = \frac{\sum M_i \cdot N_i}{Mn \cdot S_{pore}} \quad (3)$$

where $\sum M_i N_i$ (g/mol) and $\sum N_i$ represent the total mass and the number of the grafted polymer on the pore surface, respectively. S_{pore} (nm^2) is the area of the pore surface. In this analysis, the filling ratio of the fabricated PC(NIPAM) membranes was varied from 0 to 60%.

3. Results and discussion

3.1. Fabrication of the thermal-responsive gating membrane

Grafting of the NIPAM polymer onto the PC substrate was confirmed by the weight difference measured before and after graft polymerization, and also by FT-IR spectra and SEM images. In Fig. 2, the FT-IR spectra of the fabricated PC(NIPAM) membranes are shown along with the peaks of Amide I (1650 cm^{-1}) and Amide II (1550 cm^{-1}) derived from NIPAM increased as the filling ratio of the fabricated membrane increased. The filling ratio of the fabricated membranes was also confirmed to correlate with the peak ratio of P1 (Amide I at 1650 cm^{-1} derived from NIPAM) per P2 (Carbonyl stretching vibration at 1770 cm^{-1} derived from the PC substrate). The SEM images in the dry state of the PC(NIPAM) membranes with various filling ratios are shown in Fig. 3. It can be seen that the pore size of the membrane becomes smaller as the filling ratio increases. With a filling ratio of 65%, the pores, even in their dry state, were almost completely filled with grafted NIPAM

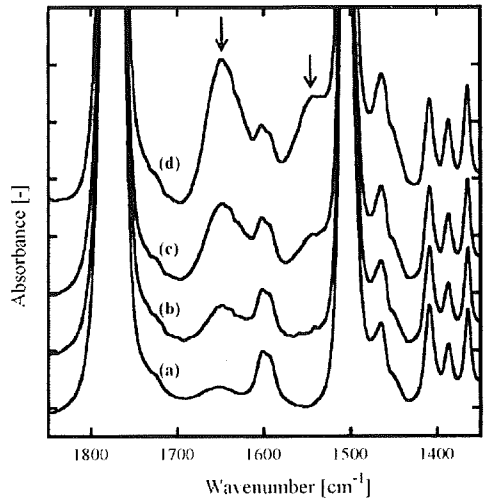

Fig. 2. FT-IR spectrum of PC(NIPAM) membrane with filling ratios: (a) PC substrate, (b) 9%, (c) 29%, and (d) 65%; the right arrow indicates the peak of Amide I and the left arrow indicates Amide II derived from NIPAM, respectively.

polymers. These results showed the grafting of the NIPAM polymer onto the pore surface of the PC substrate by plasma-induced graft polymerization.

3.2. Measurement of the water permeability through the thermal-responsive gating membrane

Fig. 4i shows the results of the permeability coefficient for pure water using a thermal-responsive gating membrane in a temperature range from 20 to 50 °C. Gating membranes with a filling ratio of 9%, 25%, 34%, and 65% were used.

At the filling ratios of 9%, 25%, and 34%, a lower critical solution temperature (LCST) was clearly observed, and the water permeation flux drastically changed because of the swelling–shrinking behavior of the grafted NIPAM polymer in the membrane pores at the LCST. In particular, the change at the LCST was several hundredfold at the filling ratio of 25%. Subsequently, it was also observed that the permeability below the LCST was almost same as that above the LCST at a filling ratio of 65%.

Moreover, the characteristic dependence of the permeation flux on the filling ratio can also be seen in Fig. 4ii. The figure also shows the maximum permeability above the LCST and the minimum below the LCST for various filling ratios. Initially, the permeability above the LCST at filling ratios from 0% (nongrafted porous substrate) to *ca.* 20% was nearly unchanged; it decreased at filling ratios above 20%. This result indicates that the pores were open nearly equal to the pore size of the nongrafted porous substrate, in spite of the grafting of the NIPAM polymer onto the pore surface. Next, the permeability below the LCST decreased dramatically for filling ratios up to *ca.* 10% and decreased gradually for filling ratios above 10%; indicating that the pores were almost closed at a filling ratio of *ca.* 10%. This means that although the pores were fully opened above the LCST at a filling ratio of *ca.* 10% because of a small amount of grafted NIPAM polymer on the pore surface, the pores were almost closed below the LCST by a small amount of swollen NIPAM polymer. Surprisingly, both of these characteristics were simultaneously accomplished at the filling ratio of *ca.* 10%; thus, the change in the permeability at the LCST increased drastically by a hundredfold. However, the reason for the characteristic dependence of the permeation flux on the filling ratio has not been clarified. This is because this characteristic dependence must be attributed largely to the properties of the grafted polymer. Therefore, it is essential to clarify the permeation behavior in order to evaluate the properties of the grafted polymer on the pore surface.

3.3. Isolation and analysis of the grafted NIPAM polymer on a polycarbonate substrate

3.3.1. Isolation of the grafted NIPAM polymer on a polycarbonate substrate

The total amount of grafted NIPAM polymer on the PC substrate, measured in Section 3.1, includes information on the molecular weight, its distribution, and the chain density of the grafted polymer. Thus, the grafted polymer was isolated from the PC substrate to evaluate the grafted polymer's properties, as shown in Scheme 2. Fig. 5 shows photographs of nontreated PC substrate (left) and PC(NIPAM) (right) for various degradation times. The filling ratio

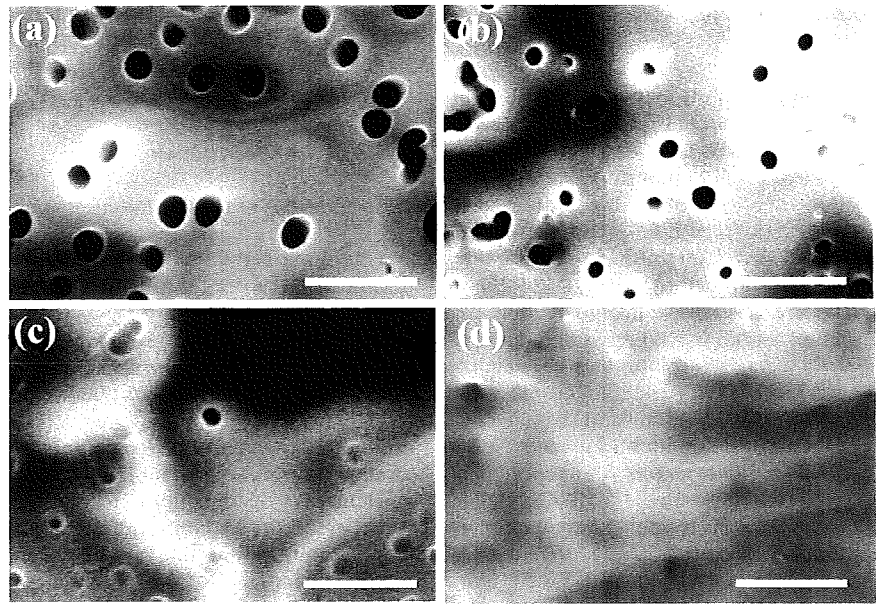

Fig. 3. SEM image of the surface of PC(NIPAM) membrane with filling ratios: (a) PC substrate, (b) 9%, (c) 29%, and (d) 65%; bar scale = 1 μm.

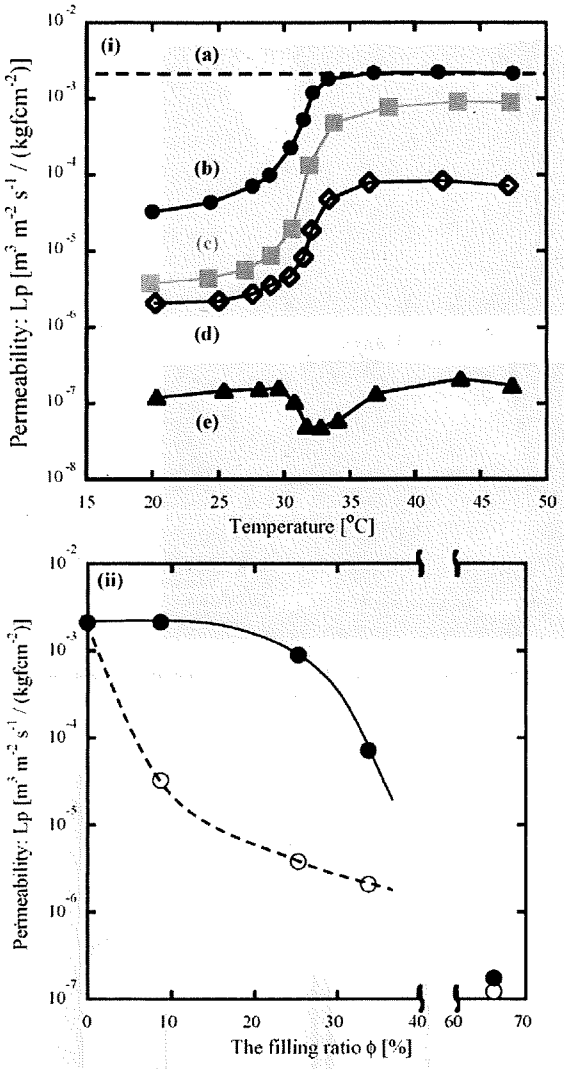

Fig. 4. (i) Permeability coefficient (L_p) of a thermal-responsive gating membrane with various filling ratios: (a) 0% (PC substrate), (b) 9%, (c) 25%, (d) 34%, and (e) 65%; and (ii) (filled circle) the value at 47 °C above the LCST and (open circle) the value at 20 °C below the LCST of L_p in various filling ratios.

of the PC(NIPAM) was 58%. It was observed that the PC substrate degraded with time, due to the hydrolysis of the ester bond of polycarbonate in a strong-alkaline and high-temperature solution. We also found that the degradation of the PC(NIPAM) was slower than that of the nontreated PC substrate. A possible reason was that the alkaline solution penetrated more slowly inside the PC(NIPAM) membrane because of the coating of NIPAM polymer on the membrane surface. After degrading for 3 days, the PC substrates were degraded and the PC substrate residues were dissolved, in the case of both the nontreated PC substrate and the PC(NIPAM). However, as shown in Fig. 5iv, the insoluble solid was observed only in the case of the PC(NIPAM). The ^{1}H NMR spectrum of the solid obtained after washing is shown in Fig. 6. From the NMR spectrum in Fig. 6, the solid was identified as a NIPAM polymer. (^{1}H NMR characteristics of grafted NIPAM polymer (in Dimethyl Sulfoxide-*d6*) are as follows: δ (ppm): (a) 0.8–1.2 (6H, CH_3 of isopropyl group), (b and c) 1.2–2.2 (3H, CH_2–CH of polymer backbone), (d) 3.7–4.0 (1H, CH of isopropyl group), and (e) 7.0–7.8 (1H, NH of amide group)). The grafted NIPAM polymer was precipitated due to the salting-out in a strong-alkaline solution. Moreover, no peak derived from a polycarbonate substrate was observed in the ^{1}H NMR spectrum of Fig. 6; thus, we found that the obtained grafted NIPAM polymer included hardly any PC substrate residue.

Subsequently, the PC substrate residue was recovered from the filtered solution, according to Scheme 2. Fig. 7 shows the ^{1}H NMR spectrum of the obtained PC substrate residue. The NMR spectrum of the obtained PC substrate residue was the same as that of bisphenol A, which is a monomer unit of polycarbonate. (^{1}H NMR characteristics of PC substrate residue (in Dimethyl Sulfoxide-*d6*) are as follows: δ (ppm): (a) 1.46–1.60 (6H, CH_3 of methyl group), (b) 6.61–6.69 and 6.94–7.02 (6H, CH of aromatic group), and (c) 9.15–9.20 (1H, OH of hydroxy group)). Thus, the PC substrate was almost completely degraded to monomer units. Moreover, the PC substrates before and after degradation were evaluated by GPC measurement, using two series of Shodex Asahipak GF-7M HQ columns. The peak of the PC substrate before degradation was observed from 20 to 35 min of retention time in the GPC chromatograph in Fig. 8. The molecular weight at the peak-top (Mp) of the PC substrate, calculated by a standard curve, was *ca.* 5.4×10^4 g/mol. On the other hand, the Mp of the PC substrate residue at 36 min of retention time was several hundred. The molecular weight of the monomer unit (bisphenol A) of polycarbonate is 228 g/mol. Thus, it was confirmed that the PC substrate had degraded to one or a few monomer units by the hydrolysis of the ester bond. We considered that the PC substrate chemically bonded to the root of the grafted NIPAM polymer was almost completely degraded; thus, the PC substrate residue in the root of the grafted polymer could not affect the properties of the grafted polymer.

3.3.2. Analysis of a grafted NIPAM polymer on a polycarbonate substrate

The above results confirmed that the grafted NIPAM polymer was isolated from the PC substrate using the evaluation method shown in Scheme 2. Then, the PC(NIPAM) membranes were used at filling ratios of 9%, 21%, and 58%, near the filling ratio used in the permeation test to clarify the permeation behavior in Section 3.2. Grafted NIPAM polymers were isolated according to Scheme 2, and evaluated by GPC measurement using two coupled columns (Shodex Asahipak GF-7M HQ and KD-806M) for the analysis of the higher molecular weight polymer.

Fig. 9i shows the results of the GPC chromatograph of a grafted NIPAM polymer isolated from various PC(NIPAM) membranes. In the chromatographs of Fig. 9i, the grafted NIPAM polymer peaked at the retention time of 22–36 min. The molecular number of grafted polymers per one pore was calculated by the results of Fig. 9i; its relationship to the molecular weight is shown in Fig. 9ii. The properties of grafted NIPAM polymers are summarized in Table 1. These results revealed several interesting points about the properties of grafted NIPAM polymers on the pore surface. First, it was found that the grafted polymer has polydispersity in all PC(NIPAM) membranes. The next point is that the peak distribution changed as the filling ratio varied. Fig. 9ii clearly shows that there was a small amount of grafted polymer with a high molecular weight of a few million; the ratio of the high molecular weight polymer was relatively low with a low filling ratio. In addition, the polymer chain density was low in the filling ratio, judging by the results of Table 1. On the other hand, as the filling ratio increased, the amount of high molecular weight polymers increased. In addition, the dispersion of the grafted polymer became narrow with the increase in the filling ratio, as shown in Table 1. This can be attributed that the high molecular weight polymer might slowly grow due to the steric hindrance of shrunk NIPAM polymer in the graft polymerization occurred in the small pore. Therefore, although the low molecular weight polymer in the pore grew as the graft polymerization proceeded, the high molecular weight polymer would not grow so much. Moreover, it was confirmed from the results of Table 1 that the polymer chain density increased about twice as the filling ratio

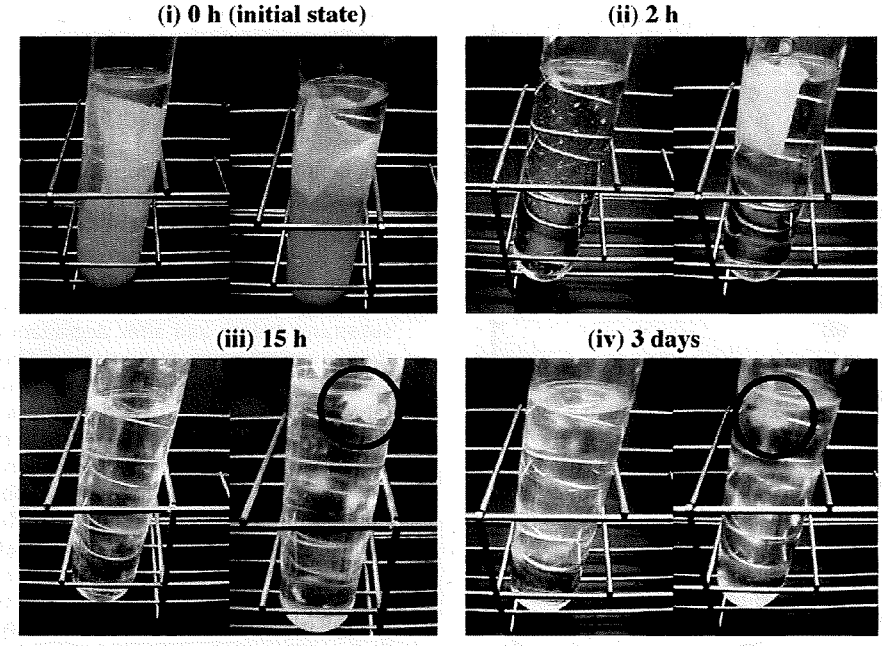

Fig. 5. Photographs of nontreated PC substrate (left) and PC(NIPAM) membrane (right) at various degradation times; the circles in (iii) and (iv) indicate the insoluble solid of grafted NIPAM polymers.

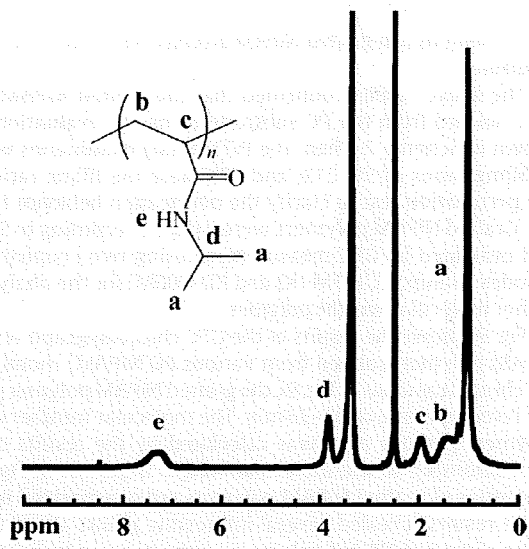

Fig. 6. NMR spectrum of a grafted NIPAM polymer at a filling ratio of 58% isolated from the PC substrate.

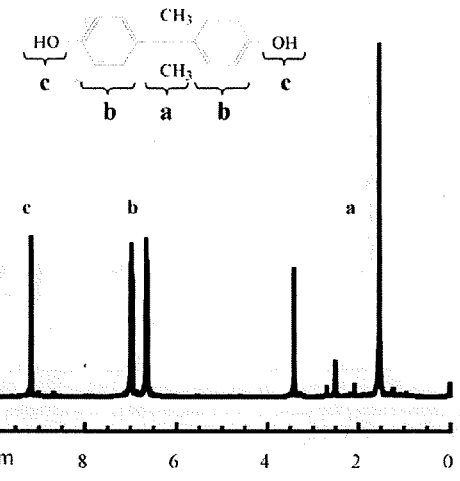

Fig. 7. NMR spectrum of the sample after degradation of the PC substrate.

increased. These results indicated that there was a little space in the membrane pore with a high filling ratio, because of the existence of a large number of high molecular weight polymers. As described above, we succeeded in evaluating the properties of the grafted polymer, chemically immobilized on the pore surface.

However, we have not yet clarified how the polydispersed grafted polymers are distributed on the pore surface. To discuss this point, the plasma-induced graft polymerization was executed using the sandwiched PC substrate. The sandwiched PC substrate can be easily used to evaluate the polymer distribution in the cross-sectional direction by peeling apart each sheet. After grafting the sandwiched PC substrate, the peak (Amide I at 1650 cm^{-1}) derived

Table 1
The properties of grafted NIPAM polymer on PC(NIPAM) membranes.

Sample	Grafting ratio[a] (%)	Mw[b] ($\times 10^4$ g mol^{-1})	Mn[c] ($\times 10^4$ g mol^{-1})	Mw/Mn	Polymer chain density[d] (chains nm^{-2})
PC(NIPAM)-1	9	120	27	4.3	0.010
PC(NIPAM)-2	21	170	51	3.3	0.012
PC(NIPAM)-3	58	210	82	2.5	0.020

[a] Calculated by Eq. (1).
[b] Weight average molecular weight (Mw) calculated by GPC chromatograph in Fig. 9i.
[c] Number average molecular weight (Mn) calculated by GPC chromatograph in Fig. 9i.
[d] Calculated by Eq. (3).

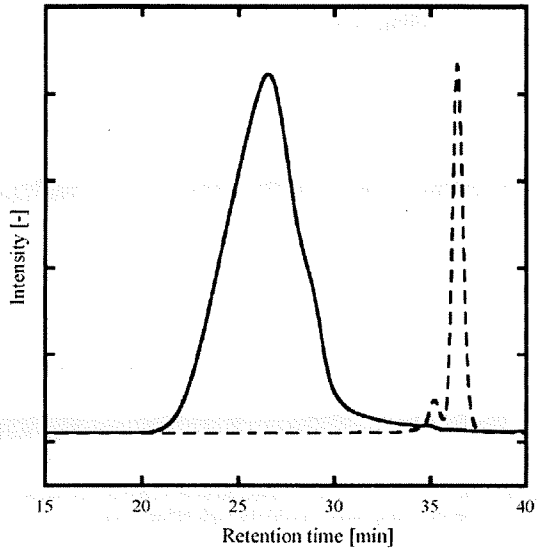

Fig. 8. GPC chromatograph of samples before (solid line) and after (dotted line) degradation of the PC substrate.

from NIPAM was observed in each sheet by FT–IR analysis. Therefore, it was found that the radicals were formed inside the sheets by the plasma treatment and the NIPAM polymer was grafted into each sheet. Fig. 10i shows the relationship between the substrate location in the sandwiched PC substrate and the filling ratio of each sheet, calculated by the peak ratio of P1/P2 in the FT–IR spectra. On the other hand, Fig. 10ii shows the calculated polymer distribution in the cross-sectional direction of a single membrane, with the assumption that the polydispersity in the GPC chromatograph of PC(NIPAM)-2 is due to an orderly arrangement, from higher to lower molecular weight, of the grafted polymer from the outside surface. With this assumption, the NIPAM polymer can almost be grafted onto the outside surface, as shown in Fig. 10ii. Here, the distribution in Fig. 10i was obviously different from that in Fig. 10ii. Therefore, the polydispersity of the grafted polymer indicated in the GPC chromatograph is almost independent of the polymer distribution in the cross-sectional direction. In other words, the polydispersed grafted polymer was almost homogeneously distributed on the pore surface, irrespective of the cross-sectional direction. This result also indicates that the amount of the grafted polymer on the outer surface was very small and the assumption at Session 2.2 was reasonable.

From the above, the grafted NIPAM polymer in the membrane pore, immobilized by the plasma-induced graft polymerization technique, was schematically summarized in Fig. 11. With a low filling ratio, there were small amounts of high molecular weight polymer of a few million and the polymer chain density was low. In addition, the grafting of the NIPAM polymer with a broad molecular weight distribution (from several ten thousands to a few million) can be homogeneously distributed on the pore surface as shown in Fig. 11i. As the filling ratio increased, the amount of high molecular weight polymers became larger, and the polymer chain density approximately doubled. Thus, there was little space in the membrane pore with a high filling ratio, as shown in Fig. 11ii.

3.4. *Clarification of the relationship between the properties of the grafted polymer and the permeation behavior of the thermal-responsive gating membrane*

As mentioned in Section 3.2, the characteristic dependence of the permeation flux of the thermal-responsive gating membrane

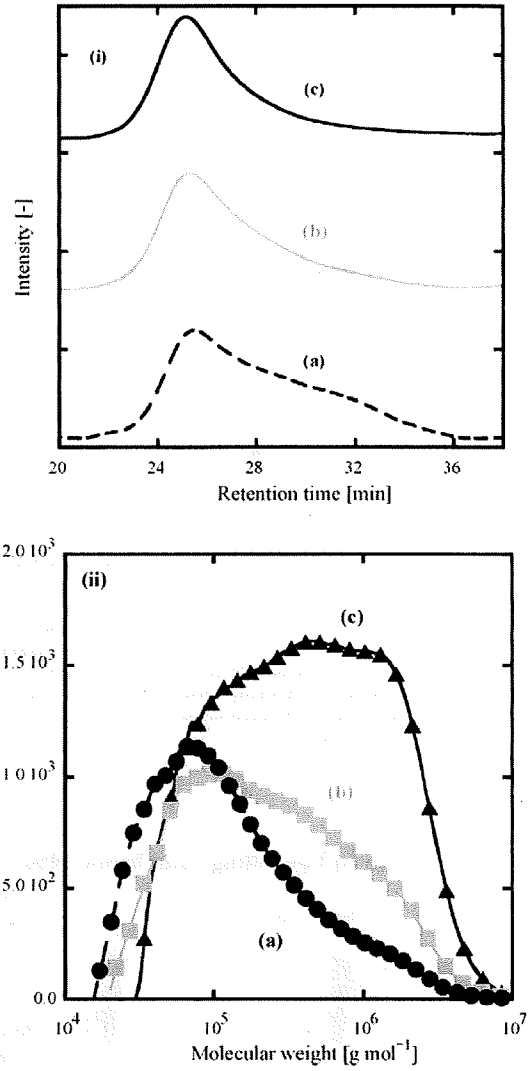

Fig. 9. GPC measurement of samples of grafted NIPAM polymer using various filling ratios: (a) 9%, (b) 21%, and (c) 58%; (i) GPC chromatograph, and (ii) molecular number of grafted NIPAM polymers per one pore.

on the filling ratio was observed. The relationship between this permeation behavior and the properties of the grafted NIPAM polymer is discussed below.

First, the permeability above the LCST, where the NIPAM polymer is in a shrunken state, with a filling ratio from 0% (nongrafted porous substrate) to *ca.* 20%, was nearly unchanged, and decreased with the filling ratio above 20%. This result indicates that the pores at this filling ratio range are open nearly equal to the pore size of the nongrafted porous substrate, in spite of the grafting of the NIPAM polymer on the pore surface. Therefore, the grafted NIPAM polymer with a filling ratio below *ca.* 20% must be fully shrunken on the pore surface when above the LCST. In other words, there can be enough space around the pore surface for shrinking the grafted polymer when above the LCST. This space around the pore surface can be formed because of the properties of the grafted polymer. Although the grafted polymer, with a filling ratio from 0% to *ca.* 20%, includes some amount of high molecular weight polymers, the polymer chain density is low. Therefore, with a filling ratio below *ca.* 20%, the grafted NIPAM polymer above the LCST was fully shrunken on the pore surface; thus the permeability was almost the same as that of a nongrafted porous substrate. As the filling ratio increased

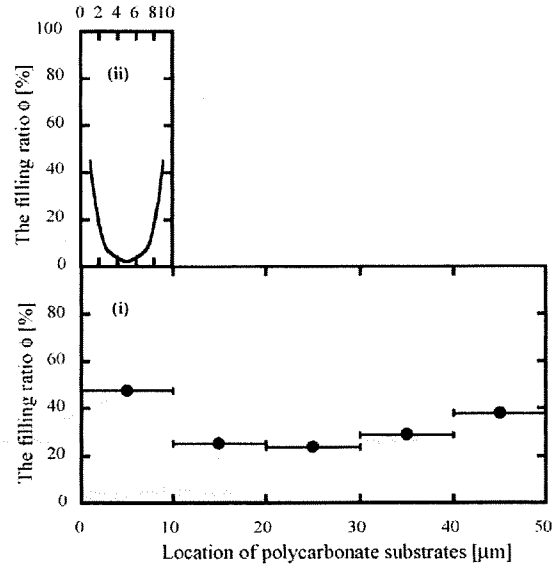

Fig. 10. (i) The relationship between substrate location in the sandwiched PC substrate and the filling ratio of grafted NIPAM polymers in each membrane; and (ii) the calculated polymer distribution in the cross-sectional direction of a single membrane, with the assumption that the polydispersity in the GPC chromatograph of PC(NIPAM)-2 is due to orderly arrangement from higher to lower molecular weight of grafted polymers from the outside surface.

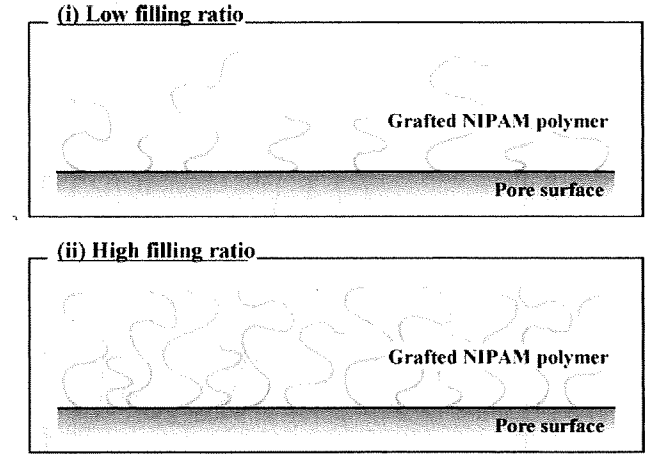

Fig. 11. Schematic illustration of grafted polymers on the pore surface of a PC substrate; (i) the low filling ratio, and (ii) the high filling ratio.

above 20%, the number of high molecular weight polymers and the polymer chain density became larger; thus there was not enough space around the pore surface for shrinking the grafted polymer when above the LCST, and the pores could not be fully opened.

Next, below the LCST, where the NIPAM polymer is in a swollen state, the permeability decreased drastically up to the filling ratio of *ca.* 10% and decreased gradually with a filling ratio above 10%. With the filling ratio below 10%, the grafted polymer with a broad molecular weight can be homogeneously distributed on the pore, and

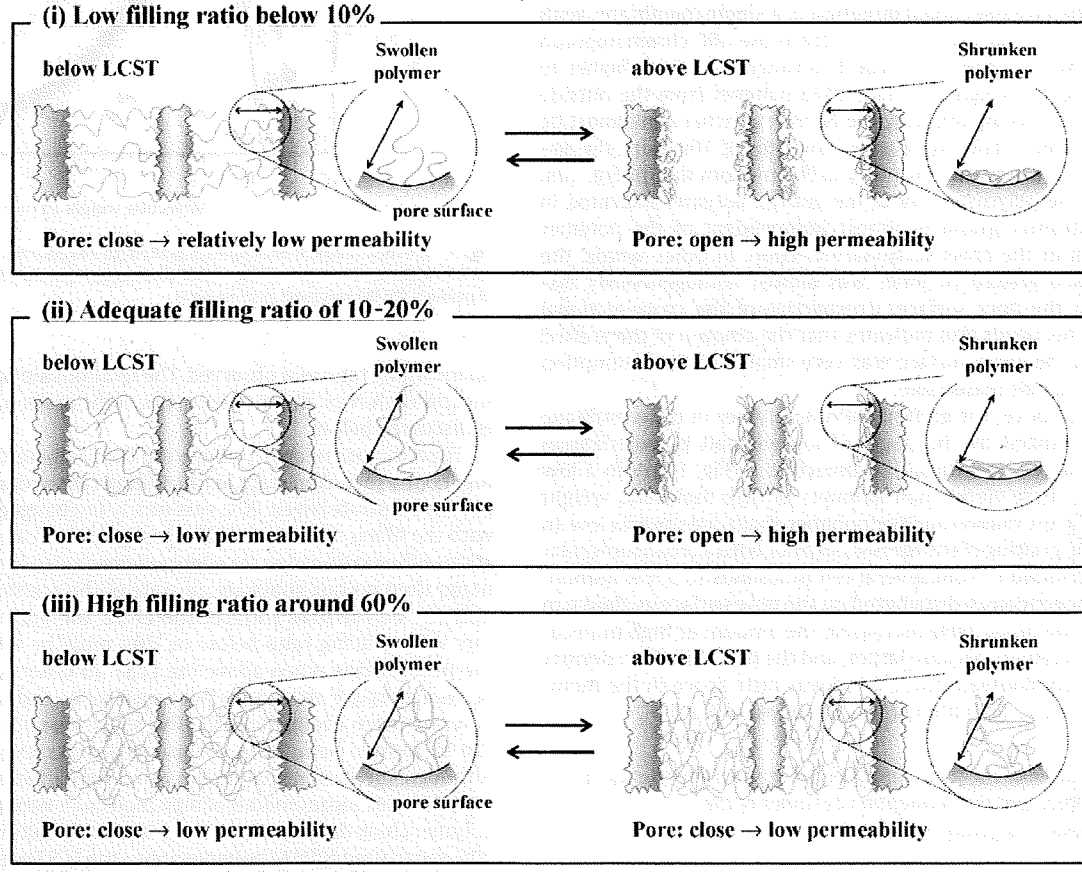

Fig. 12. Schematic illustration of the pore gating of a thermal-responsive gating membrane; (i) the low filling ratio below 10%, (ii) the adequate filling ratio of 10–20%, and (iii) the high filling ratio around 60%.

the number of high molecular weight polymers was low, from the results of Fig. 9ii. In addition, the chain density of the grafted NIPAM polymer was *ca.* 0.01 chains nm^{-2}, thus this polymer chain would belong to a semi-dilute polymer brush in which it and its neighboring grafted polymer could affect each other to some extent. It was previously reported [36] that the value of L_e/L_c, where L_e is the equilibrium thickness of the swollen brush and L_c is the full length of the graft chain in the all-trans conformation, is *ca.* 0.2 in the case of the polymer brush density of 0.01 chains nm^{-2} with a narrow polymer distribution ($Mw/Mn \approx 1$). Assuming the value of $L_e/L_c = 0.2$ in the grafted NIPAM polymer in the membrane pore, the pore with a diameter of 200 nm would be closed by a swollen NIPAM polymer above 2×10^5 molecular weight ($g\,mol^{-1}$). At the filling ratio of *ca.* 10%, the number of polymers with a molecular weight higher than $2 \times 10^5\,g\,mol^{-1}$ was low. In spite of this, the water permeability was low below the LCST, as shown in Fig. 4ii, thus the pores were almost closed by the swollen NIPAM polymer. Therefore, it can be suggested that the pores were sufficiently closed by a small amount of swollen NIPAM polymer with a high molecular weight (from several hundred thousand to a few million). In addition, the grafted polymers with a high molecular weight can entangle each other in the membrane pore. These results mean that there can be enough grafted NIPAM polymers with a high molecular weight to close the pores with a filling ratio of *ca.* 10%. Furthermore, the permeability decreased gradually at a filling ratio above 10% because the excess NIPAM polymers with a high molecular weight increased gradually.

From the above discussions, the significant factors for the drastic pore gating in a thermal-responsive gating membrane were suggested. First, for the pores to fully open nearly equal to the pore size of the nongrafted porous substrate, there must be enough space around the pore surface for a grafted NIPAM polymer to shrink. Next, the pores must be sufficiently closed below the LCST by a small amount of swollen NIPAM polymers with a high molecular weight in the membrane pore. Surprisingly, at an adequate filling ratio of 10–20%, both of these characteristics were simultaneously accomplished, owing to the properties of a grafted polymer immobilized by plasma-induced graft polymerization. At an adequate filling ratio of 10–20%, as shown in Fig. 12ii, the grafted polymer includes some quantity of low molecular weight polymers and its chain density is low. Therefore, there can be enough space around the pore surface for the grafted polymer to shrink and the pores are fully open above the LCST. On the other hand, the pores could be closed below the LCST by the entanglement of swollen NIPAM polymers, with a certain amount of high molecular weight (from several hundred thousand to a few million) in the membrane pore. Therefore, we can accomplish the drastic change in water permeability at the LCST by several hundredfold.

Furthermore, we can explain the permeation behavior of the thermal-responsive gating membrane at various filling ratios by the properties of the grafted polymer. At a low filling ratio below 10%, the number of high molecular weight polymers was lower, compared with an adequate filling ratio; thus the pores were not fully closed below the LCST and they were open above the LCST, as shown in Fig. 12i. Conversely, at a filling ratio above 20%, the number of high molecular weight polymers and the polymer chain density becoming larger compared with an adequate filling ratio, there cannot be enough space around the pore surface for the grafted polymer to shrink above the LCST. Eventually, at a high filling ratio around 60%, there can be little space in the membrane pore for changing the volume of grafted NIPAM polymers at the LCST. Therefore, the membrane pores were almost closed whether the grafted NIPAM polymer was swollen or not, as shown in Fig. 12iii. In our previous report, the water content (the solubility to a grafted polymer) in a pore-filling membrane (the pores are completely filled at near 100%) can largely influence a membrane permeability [27]. We considered that the water permeability at a filling ratio around 60% can be attributed to both of the pore gating and the water content. Therefore, at the filling ratio of 65%, the change of the permeability around the LCST (30–35 °C) as shown in Fig. 4i was obtained.

4. Conclusions

In this study, we successfully clarified the relationship between the properties of a grafted NIPAM polymer in the membrane pore and the permeation behavior of thermal-responsive gating membranes, as described in details below.

Thermal-responsive gating membranes were fabricated by grafting a NIPAM polymer onto a straight cylindrical pore of a polycarbonate porous substrate by plasma-induced graft polymerization. In this gating membrane, we obtained a drastic change in water permeability at the LCST. Moreover, the characteristic dependence of the permeation flux on the filling ratio was also observed. The permeability above the LCST with a filling ratio from 0% (nongrafted porous substrate) to *ca.* 20% was nearly unchanged, and later, it decreased with a filling ratio above 20%. Next, the permeability below the LCST decreased dramatically with a filling ratio up to *ca.* 10%, and decreased gradually with a filling ratio above 10%. To clarify this permeation behavior, the properties of the grafted polymer are evaluated.

By the hydrolysis of the ester bond of polycarbonate in a strong-alkaline, high-temperature solution, the grafted NIPAM polymer was isolated from a polycarbonate substrate, and its properties were evaluated. These evaluations revealed unique characteristics of the grafted NIPAM polymer. First, the NIPAM polymer with a broad molecular weight distribution (from several ten thousands to a few million) was almost homogeneously grafted on the pore surface and the polymer chain density was low. Next, the amount of high molecular weight polymers becomes larger, and the polymer chain density increases as the filling ratio increases.

From these results, we clarified the relationship between the properties of the grafted polymer in the membrane pore and the permeation behavior of the thermal-responsive gating membrane for the first time. First, in the case of above the LCST, the pores were fully open at a filling ratio below 20%, nearly equal to the pore size of the nongrafted porous substrate, by the existence of enough space around the pore surface for the grafted NIPAM polymer to shrink. At a filling ratio below 20%, the grafted polymer includes some low molecular weight polymers and its chain density is low; thus, there can be enough space around the pore surface to shrink the grafted polymer. Therefore, the pores were fully open above the LCST, and the permeability at a filling ratio from 0% to *ca.* 20%, was nearly unchanged. In addition, when the filling ratio was above 20%, the number of high molecular weight polymers and the polymer chain density increased; thus, the space around the pore surface was not enough for the grafted polymer to shrink above the LCST. Next, in the case of below the LCST, the pores were sufficiently closed at a filling ratio of *ca.* 10% by the entanglement of swollen NIPAM polymers with a small amount of high molecular weight polymers in the membrane pore. In addition, the permeability decreased gradually with a filling ratio above 10% because excess NIPAM polymers with a high molecular weight increased gradually. Therefore, at an adequate filling ratio of 10–20%, we can accomplish a drastic change in the water permeability at the LCST, owing to the abovementioned characteristics of the grafted polymer.

From the above, we suggest that the permeation behavior in the gating membrane is strongly related to the properties of the grafted polymer. The knowledge obtained in this study can provide useful information for designing the gating function in a stimuli-responsive gating membrane. We also believe that the methodology proposed in this study can be applied to other grafting techniques and prove useful in clarifying their microscopic phenomena.

Acknowledgements

This work was supported in part by the Global COE Program, "Chemistry Innovation through Cooperation of Science and Engineering," MEXT, Japan. We also thank the Kohjin Co. for supplying NIPAM and Ms. Yumi Ogino for supplying some thermal-responsive gating membranes.

References

[1] H. Iwata, M. Oodate, Y. Uyama, H. Amemiya, Y. Ikada, Preparation of temperature-sensitive membranes by graft-polymerization onto a porous membrane, J. Membr. Sci. 55 (1991) 119.
[2] Y.S. Park, Y. Ito, Y. Imanishi, Permeation control through porous membranes immobilized with thermosensitive polymer, Langmuir 14 (1998) 910.
[3] T. Peng, Y.L. Cheng, Temperature-responsive permeability of porous PNIPAAm-g-PE membranes, J. Appl. Polym. Sci. 70 (1998) 2133.
[4] L. Liang, M.K. Shi, V.V. Viswanathan, L.M. Peurrung, J.S. Young, Temperature-sensitive polypropylene membranes prepared by plasma polymerization, J. Membr. Sci. 177 (2000) 97.
[5] N.I. Shtanko, V.Y. Kabanov, P.Y. Apel, M. Yoshida, A.I. Vilenskii, Preparation of permeability-controlled track membranes on the basis of 'smart' polymers, J. Membr. Sci. 179 (2000) 155.
[6] R. Xie, L.Y. Chu, W.M. Chen, W. Xiao, H.D. Wang, J.B. Qu, Characterization of microstructure of poly (*N*-isopropylacrylamide)-grafted polycarbonate track-etched membranes prepared by plasma-graft pore-filling polymerization, J. Membr. Sci. 258 (2005) 157.
[7] E.C. Muniz, G. Geuskens, Influence of temperature on the permeability of polyacrylamide hydrogels and semi-IPNs with poly(*N*-isopropylacrylamide), J. Membr. Sci. 172 (2000) 287.
[8] S.J. Lue, J.J. Hsu, C.H. Chen, B.C. Chen, Thermally on-off switching membranes of poly(*N*-isopropylacrylamide) immobilized in track-etched polycarbonate films, J. Membr. Sci. 301 (2007) 142.
[9] I. Lokuge, X. Wang, P.W. Bohn, Temperature-controlled flow switching in nanocapillary array membranes mediated by poly(*N*-isopropylacrylamide) polymer brushes grafted by atom transfer radical polymerization, Langmuir 23 (2007) 305.
[10] P.F. Li, R. Xie, J.C, Jiang, T. Meng, M. Yang, X.J. Ju, L.H. Yang, L.Y. Chu, Thermo-responsive gating membranes with controllable length and density of poly(*N*-isopropylacrylamide) chains grafted by ATRP method, J. Membr. Sci. 337 (2009) 310.
[11] G.J. Liu, Z.H. Lu, S. Duncan, Porous membranes of polysulfone-graft-poly(tert-butyl acrylate) and polysulfone-graft-poly(acrylic acid): morphology, pH-gated water flow, size selectivity, and ion selectivity, Macromolecules 37 (2004) 4218.
[12] I. Tokarev, M. Orlov, S. Minko, Responsive polyelectrolyte gel membranes, Adv. Mater. 18 (2006) 2458.
[13] A.M. Mika, R.F. Childs, J.M. Dickson, B.E. McCarry, D.R. Gagnon, A new class of polyelectrolyte-filled microfiltration membranes with environmentally controlled porosity, J. Membr. Sci. 108 (1995) 37.
[14] Y.M. Lee, S.Y. Ihm, J.K. Shim, J.H. Kim, C.S. Cho, Y.K. Sung, Preparation of surface-modified stimuli-responsive polymeric membranes by plasma and ultraviolet grafting methods and their riboflavin permeation, Polymer 36 (1995) 81.
[15] Y. Ito, Y.S. Park, Y. Imanishi, Visualization of critical pH-controlled gating of a porous membrane grafted with polyelectrolyte brushes, J. Am. Chem. Soc. 119 (1997) 2739.
[16] Y.S. Park, Y. Ito, Y. Imanishi, Photocontrolled gating by polymer brushes grafted on porous glass filter, Macromolecules 31 (1998) 2606.
[17] Y. Ito, S. Nishi, Y.S. Park, Y. Imanishi, Oxidoreduction-sensitive control of water permeation through a polymer brushes-grafted porous membrane, Macromolecules 30 (1997) 5856.
[18] K. Ishihara, M. Kobayashi, N. Ishimaru, I. Shinohara, Glucose-induced permeation control of insulin through a complex membrane consisting of immobilized glucose-oxidase and a poly(amine), Polymer J. 16 (1984) 625.
[19] L.Y. Chu, Y. Li, J.H. Zhu, H.D. Wang, Y.J. Liang, Control of pore size and permeability of a glucose-responsive gating membrane for insulin delivery, J. Control Rel. 97 (2004) 43.
[20] T. Ito, T. Hioki, T. Yamaguchi, T. Shinbo, S. Nakao, S. Kimura, Development of a molecular recognition ion gating membrane and estimation of its pore size control, J. Am. Chem. Soc. 124 (2002) 7840.
[21] T. Ito, T. Yamaguchi, Osmotic pressure control in response to a specific ion signal at physiological temperature using a molecular recognition ion gating membrane, J. Am. Chem. Soc. 126 (2004) 6202–6203.
[22] T. Ito, T. Yamaguchi, Controlled release of model drugs through a molecular recognition ion gating membrane in response to a specific ion signal, Langmuir 22 (2006) 3945.
[23] M. Ulbricht, Advanced functional polymer membranes, Polymer 47 (2006) 2217–2262.
[24] Z.M.O. Rzaev, S. Dincer, E. Piskin, Functional copolymers of *N*-isopropylacrylamide for bioengineering applications, Prog. Polym. Sci. 32(2007) 534.
[25] A. Friebe, M. Ulbricht, Cylindrical pores responding to two different stimuli via surface-initiated atom transfer radical polymerization for synthesis of grafted diblock copolymers, Macromolecules 42 (2009) 1838.
[26] H. Yasuda, Plasma for modification of polymers, J. Macromol. Sci. Chem. 10 (1976) 383.
[27] T. Yamaguchi, S. Nakao, S. Kimura, Plasma-graft filling polymerization—preparation of a new type of pervaporation membrane for organic liquid-mixtures, Macromolecules 24 (1991) 5522.
[28] M. Ulbricht, G. Belfort, Surface modification of ultrafiltration membranes by low temperature plasma. II. Graft polymerization onto polyacrylonitrile and polysulfone, J. Membr. Sci. 111 (1996) 193.
[29] T. Yamaguchi, S.I. Nakao, S. Kimura, Evidence and mechanisms of filling polymerization by plasma-induced graft polymerization, J. Polym. Sci. Pol. Chem. 34 (1996) 1203.
[30] Y.J. Choi, S.H. Moon, T. Yamaguchi, S.I. Nakao, New morphological control for thick, porous membranes with a plasma graft-filling polymerization, J. Polym. Sci. Pol. Chem. 41 (2003) 1216.
[31] T. Kai, W. Ueno, T. Yamaguchi, S.I. Nakao, Role of vacuum ultraviolet irradiation in plasma-induced graft polymerization in the pore-filling polymerization of porous materials, J. Polym. Sci. Pol. Chem. 43 (2005) 2068.
[32] T. Kai, Y. Suma, S. Ono, T. Yamaguchi, S.I. Nakao, Effect of the pore surface modification of an inorganic substrate on the plasma-grafting behavior of pore-filling-type organic/inorganic composite membranes, J. Polym. Sci. Pol. Chem. 44 (2006) 846–856.
[33] Y. Hirokawa, T. Tanaka, Volume phase-transition in a nonionic gel, J. Chem. Phys. 81 (1984) 6379.
[34] H. Yamagishi, K. Saito, S. Furusaki, T. Sugo, F. Hosoi, J. Okamoto, Molecular-weight distribution of methyl-methacrylate grafted onto a microfiltration membrane by radiation-induced graft-polymerization, J. Membr. Sci. 85 (1993) 71.
[35] M. Chaimberg, Y. Cohen, Free-radical graft-polymerization of vinylpyrrolidone onto silica, Ind. Eng. Chem. Res. 30 (1991) 2534.
[36] S. Yamamoto, M. Ejaz, Y. Tsujii, T. Fukuda, Surface interaction forces of well-defined, high-density polymer brushes studied by atomic force microscopy. 2. Effect of graft density, Macromolecules 33 (2000) 5608.

Journal of Membrane Science 348 (2010) 369–375

Contents lists available at ScienceDirect

Journal of Membrane Science

journal homepage: www.elsevier.com/locate/memsci

Reentrant phase transition behavior and sensitivity enhancement of a molecular recognition ion gating membrane in an aqueous ethanol solution

Taichi Ito [b], Yuhei Oshiba [a,1], Hidenori Ohashi [a,1], Takanori Tamaki [a,1], Takeo Yamaguchi [a,*]

[a] Chemical Resources Laboratory, Tokyo Institute of Technology, 4259 Nagatsuta, Midori-ku, Yokohama 226-8503, Japan
[b] Center for Disease Biology and Integrative Medicine, Department of Chemical System Engineering, The University of Tokyo, 7-3-1 Bunkyo-ku, Hongo, Tokyo 113-0033, Japan

ARTICLE INFO

Article history:
Received 7 August 2009
Received in revised form
11 November 2009
Accepted 14 November 2009

Keywords:
Molecular recognition
Gating membrane
Crown ether
N-isopropylacrylamide

ABSTRACT

The response behavior of a molecular recognition ion gating membrane to an ion signal was investigated in an aqueous ethanol solution. The linear poly-*N*-isopropylacrylamide (NIPAM)-co-benzo[18]-crown-6-acrylamide (BCAm) copolymer showed phase separation in response to variation in ethanol mole fraction in the mixed solvent of water and ethanol, which is called a reentrant coil-to-globule-to-coil transition. The phase diagram of poly-NIPAM-co-BCAm changed in response to the concentration of a specific ion signal. Based on this reentrant phase transition behavior of the copolymer, the gating membrane, which was prepared by grafting the copolymer of NIPAM and BCAm onto the surface of a porous polyethylene film, opened and closed its pores by the swelling and shrinking of the grafted copolymer in an aqueous ethanol solution. In addition, the complex formation constant of BCAm increased with increasing ethanol mole fraction, which enhanced the response sensitivity and selectivity to ion species; thus, the sensitivity to $BaCl_2$ was 10 times higher in 19.6 mol% aqueous ethanol solution than it was in pure water.

1. Introduction

Biomembranes are highly functional but too unstable for engineering use. On the other hand, synthetic membranes are stable, but do not have high functionality such as responsiveness to environmental conditions. Inspired by the functions of ion channels embedded in a biomembrane, we have developed a molecular recognition ion gating membrane in which the copolymer of poly-NIPAM-co-BCAm was grafted onto the surface of a porous polyethylene film. The phase transition of the grafted copolymer repeatedly occurs in the pores in response to an ion signal; hence, the gating membrane spontaneously controlled pressure-driven flow [1], solute rejection [1], and osmotic pressure [2] by changing the diameter of the nanosized pores in response to a specific ion signal such as K^+ and Ba^{2+} in water, like the ion channels of biomembranes (Fig. 1). We recently reported that this membrane triggered nonlinear oscillation with switching between osmotic flow and hydrostatic pressure-driven flow without any external stimuli, like an excitation of neurons consisting of many ion channels [3]. In addition, other groups have reported various types of gating membrane in response to environmental conditions such as pH and temperature [4–14].

Compared with ion channels of biomembranes consisting of proteins, our gating membrane can be extremely stable because both substrate porous film and grafted copolymer are synthetic polymers that are extremely stable in organic solvents such as alcohols. Therefore, its stable and reversible reaction can be expected even in organic solvents and/or mixtures of organic solvent and water. In fact, such a membrane is important and needed in various processes such as ethanol production by fermentation. Thus, we reported the function of poly-NIPAM-grafted membrane to respond to ethanol concentration [36]. The concentration of various ions varies during fermentation; hence, the concentration needs to be monitored. The concentration of many materials should also be controlled in the formation process in response to an external ion concentration. For these purposes, it is important to investigate the response behavior of the gating membrane in a mixed solvent of ethanol and water. However, even the phase separation behavior of poly-NIPAM-co-BCAm has not been reported.

Poly-NIPAM and its gel show cononsolvency in water–alcohol mixed solvents such as methanol and ethanol [15–25]. For instance, poly-NIPAM is in a coil state in pure water, transitions into a globule state at a certain concentration of methanol in the mixture of water and methanol, and goes back to a coil state at high methanol concentration with increase in alcohol concentration at a constant temperature. That is, water and methanol themselves are good solvents for poly-NIPAM, but their mixture becomes a poor solvent

* Corresponding author at: Chemical Resources Laboratory, Tokyo Institute of Technology, R1-17, 4259 Nagatsuta, Midori-ku, Yokohama 226-8503, Japan.
Tel.: +81 45 924 5254; fax: +81 35 841 5262.
E-mail address: yamag@res.titech.ac.jp (T. Yamaguchi).
[1] Tel.: +81 45 924 5254; fax: +81 35 841 5262.

0376-7388/$ – see front matter © 2009 Elsevier B.V. All rights reserved.
doi:10.1016/j.memsci.2009.11.028

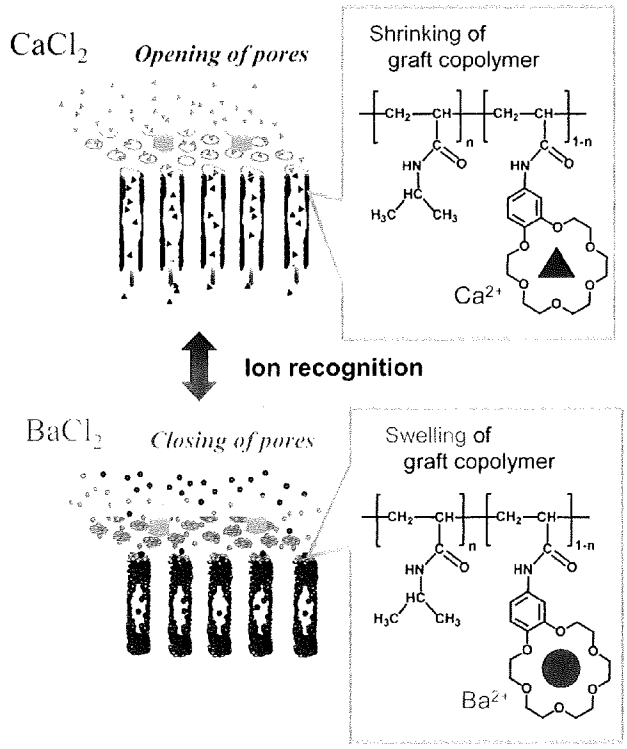

Fig. 1. Concept of a molecular recognition ion gating membrane made of porous PE-g-NIPAM-co-BCAm.

for poly-NIPAM. This is called cononsolvency or a reentrant coil-to-globule-to-coil transition. The reentrant phase transition causes a poly-NIPAM gel to undergo a reentrant volume phase transition in an aqueous alcohol solution.

Although this reentrant phase transition of poly-NIPAM has been well known for a long time, its mechanism is still discussed and is an interesting topic [31–35]. Poly-NIPAM shows two types of reentrant phase transitions, which have two lower critical solution temperatures (LCSTs) or a combination of an LCST and an upper critical solution temperature (UCST) [20,25]. However, to the best of our knowledge, the phase transition behavior of poly-NIPAM-co-BCAm has been reported in pure water only [26], and not in the mixed solvent of water and organic solvent system. When BCAms are introduced into poly-NIPAM, complex formation between BCAm and a signal ion may affect the behavior of water and ethanol molecules, and vice versa. That is to say, the complex formation phenomenon can also change the reentrant phase transition in an aqueous ethanol solution in a molecular recognition manner.

In the present research, we report for the first time the phase transition behavior of linear poly-NIPAM-co-BCAm in aqueous ethanol solution in the presence or absence of ion signals. Following that, the response behavior of pressure-driven flow through the molecular recognition ion gating membrane in response to signal ion species and their concentration, ethanol concentration and temperature were investigated in an aqueous ethanol solution.

2. Experimental

2.1. Poly-NIPAM-co-BCAm preparation and its turbidity measurement

BCAm was synthesized according to the reported procedures [27,28]. Both NIPAM and BCAm were recrystallized from benzene. Poly-NIPAM-co-BCAm was synthesized using radical copolymerization in distilled tetrahydrofuran using 0.3 mol% azobisisobutyronitrile as the initiator at 70 °C according to the method used previously [29]. The mole ratio of NIPAM to BCAm in the monomer solution was 95:5, which is equal to 85:15 as a weight ratio. The concentration of the monomer solution was 25 wt%. The synthesized copolymer was dissolved in a mixture of water, ethanol at 0.1 wt%, and/or ions such as $BaCl_2$ or $CaCl_2$, and its turbidity was measured by the absorbance of visible light at 650 nm using UV–vis spectroscopy (Hitachi U-3300). The measurement temperature was varied from 0 to 70 °C.

2.2. Membrane preparation

The membrane was prepared using the peroxide plasma graft polymerization method, as described in our earlier publications [1,2]. A porous polyethylene (HDPE) film (Asahi Kasei, Japan, pore size = 200 nm, thickness = 100 μm, porosity = 69%) was used as a substrate, and the plasma treatment power and time were 30 W and 1 min, respectively. The grafting amount of the membrane used in this study was 1.01 mg/cm^2. The copolymer composition of the membrane of NIPAM to BCAm was 93:7, which is the same as that of poly-NIPAM-co-BCAm [29].

2.3. Filtration experiments

The filtration experiments shown as (1)–(3) were carried out by cross-flow filtration, as described in our earlier publication [1]. A feed solution was flowed parallel to the membrane surface at a flow rate of 500 g/min, the effective membrane area being 13.2 cm^2. An applied pressure was maintained at between 0.3 and 0.5 kgf/cm^2. Instead of the solution flux, the permeability coefficient, L_p [mg/(cm^2 s)], was used to correct for any applied pressure difference. Note that the temperature dependence of the solution viscosity was ignored.

(1) *Measurement of the ethanol concentration dependence of the solution flux. The mixture of water and ethanol containing no ion or 10 mM $BaCl_2$ solutions were filtered. The ethanol concentration was varied from* 0 to 25 mol%.
(2) *Measurement of the temperature dependence of the solution flux.* Mixtures of water and ethanol in which the ethanol concentration was 0, 19.6, or 26.1 mol% and contained no ion were filtered. Mixtures of water and ethanol in which the ethanol concentration was 19.6 mol% and contained 10 mM $BaCl_2$, $SrCl_2$, KCl, or $CaCl_2$ were also filtered. Mixtures of water and ethanol in which the ethanol concentration was 19.6 mol% and contained different concentrations of $BaCl_2$ (1, 10, 20, 30 mM) were also filtered. The solution temperature was varied from 13 to 50 °C.
(3) *Measurement of the ion concentration dependence of the solution flux.* Mixtures of water and ethanol in which the ethanol concentration was 0 or 19.6 mol% containing $BaCl_2$ or $CaCl_2$ were filtered. The ion concentration was altered from 0.1 to 50 mM. Note that the operation temperature was 39.5 °C in the case of 19.6 mol% ethanol and 27.3 °C in the case of pure water.

3. Results and discussion

3.1. Increase of LCST shift of poly-NIPAM-co-BCAm triggered by a specific ion signal with increasing ethanol concentration

Poly-NIPAM-co-BCAm was dissolved in mixed solvents made from different concentrations of ethanol and pure water. A photograph of the solutions in which the ethanol concentrations were 0, 9.3, 23.5, or 100 mol% is shown in Fig. 2. The solutions in (A), (B), (C)

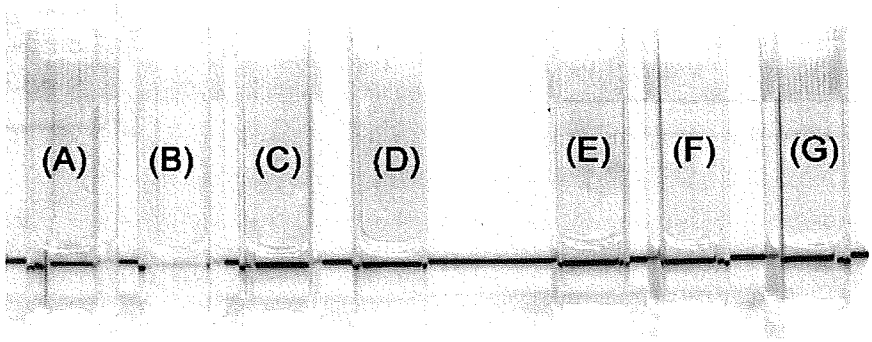

Fig. 2. Photograph of 0.1 wt% poly-NIPAM-co-BCAm showing that the solutions of varying ethanol mole ratio were different without any ion ((A)–(D)) and with 10 mM $BaCl_2$ ((E)–(G)). Ethanol concentrations were (A), (E) pure water, 0 mol%, (B), (F) 9.3 mol%, (C), (G) 23.5 mol%, (D) 100 mol%. Only (B) became cloudy.

and (D) contained no ions. The aqueous solution in (A) was homogeneous, but at 9.3 mol% in (B) became cloudy. With increasing ethanol mole ratio, 23.5 and 100 mol% in (C) and (D), respectively, the solution became homogeneous again. This is a typical reentrant phase transition behavior in which the polymer starts swelling, then shrinks with changing solvent composition, and finally swells again at a constant temperature. On the other hand, the solutions in (E), (F) and (G) contained 10 mM $BaCl_2$. Because the solubility of $BaCl_2$ decreased with increasing ethanol mole ratio, the equivalent amount of 10 mM $BaCl_2$ did not dissolve in pure ethanol. At any concentration of ethanol, the solutions of (E), (F) and (G) remained dissolved, which means that reentrant phase transition behavior disappeared because of ion addition.

The phase transition of poly-NIPAM-co-BCAm was explored in more detail by turbidity measurements. The absorbance of poly-NIPAM-co-BCAm solutions in which the ethanol concentration was different and contained 10 mM $BaCl_2$ was measured as a function of temperature, as shown in Fig. 3(A) and (B). At low ethanol concentration, phase separation occurred sharply at the LCST, as shown in Fig. 3(A), while it changed to continuous phase separation at

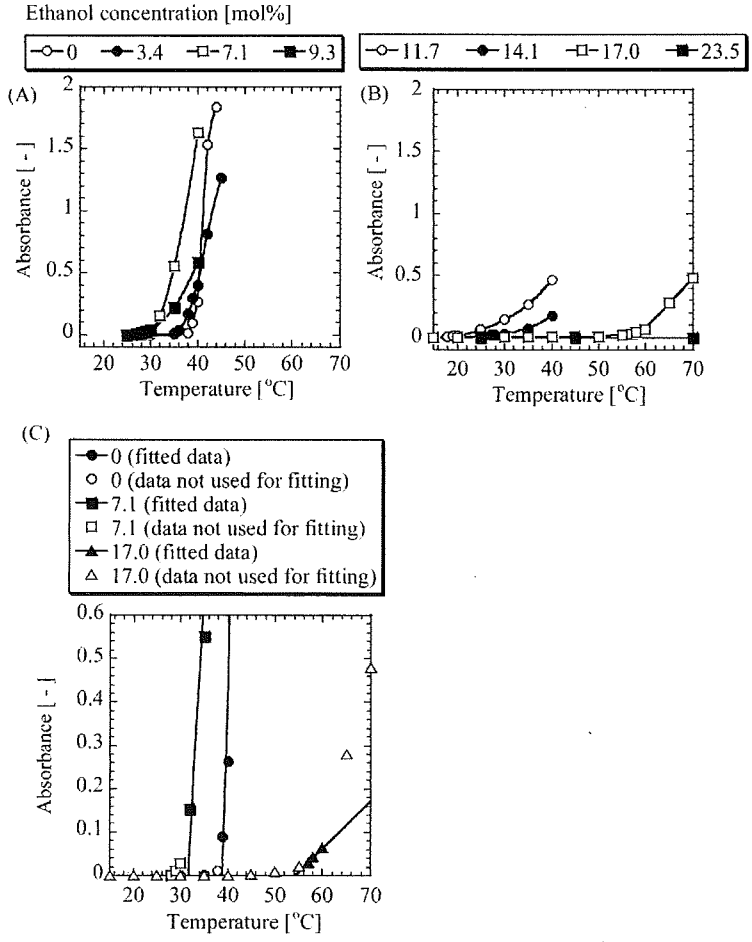

Fig. 3. Temperature dependence of the turbidity of poly-NIPAM-co-BCAm in various concentrations of aqueous ethanol solution that contained 10 mM $BaCl_2$. (A) Ethanol concentration was varied between 0 and 9.3 mol%. (B) Ethanol concentration was varied between 11.7 and 23.5 mol%. (C) LCST was defined as the x-intercept of the tangential line of each turbidity curve.

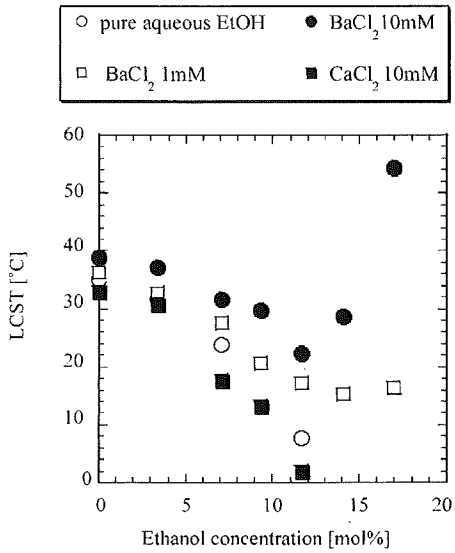

Fig. 4. Temperature–ethanol concentration phase diagram of poly-NIPAM-co-BCAm in response to signal ions. Ethanol mole ratio was varied between 0 and 20 mol%. The concentration of $BaCl_2$ was 1 and 10 mM. As a control experiment, pure solvent and 10 mM $CaCl_2$ were used.

high ethanol concentration, as shown in Fig. 3(B). Thus, the LCST was defined as the intercept temperature of the tangential line of each turbidity curve, as shown in Fig. 3(C). In addition, the LCSTs shifted to lower temperature with increasing ethanol concentration, as shown in Fig. 3(A), and then shifted oppositely to higher temperature above 11.7 mol% of ethanol, as shown in Fig. 3(B).

By determining LCSTs of poly-NIPAM-co-BCAm solution in which the analyte ion concentration is varied, the change of phase diagram in response to signal ions was obtained, as shown in Fig. 4. In the case of pure solvent or 10 mM $CaCl_2$ solution, the phase transition behavior of poly-NIPAM-co-BCAm was almost the same as that of poly-NIPAM already reported previously [19,20]. When $BaCl_2$ was added instead of $CaCl_2$, the LCST shifted higher, the shift width becoming higher with increasing ethanol concentration in the region where ethanol concentration was below ca. 12 mol%. This is probably because the complex formation constant of BCAm increased with increasing ethanol concentration [30].

3.2. Change of phase diagram and reentrant phase transition of poly-NIPAM-co-BCAm by a specific ion signal

It is reported that poly-NIPAM has an LCST at low concentrations of ethanol and a UCST at relatively high concentrations of ethanol in aqueous ethanol solutions. Between the LCST ($LCST_1$) and UCST lines, there is a globule-state region where poly-NIPAM is always insoluble at any temperature. Interestingly, the phase diagram of poly-NIPAM-co-BCAm in aqueous ethanol solution was different from that of poly-NIPAM in aqueous ethanol [20] even without adding ions. It has $LCST_1$, which we focused on in Fig. 4 and a second LCST ($LCST_2$) replaced with UCST, but there is a coil-state region of an insoluble state at any temperature.

When 10 mM $CaCl_2$ solution was used, the phase diagram was almost the same as that of pure solvent. On the other hand, in the case of $BaCl_2$, the globule-state region became smaller with increasing $BaCl_2$ concentration, and then two coil-state regions finally connected and became one region. Thus, the LCST lines became concave. As a result, the reentrant phase transition behavior of poly-NIPAM at around room temperature was lost because of the Ba^{2+} signal in the case of poly-NIPAM-co-BCAm.

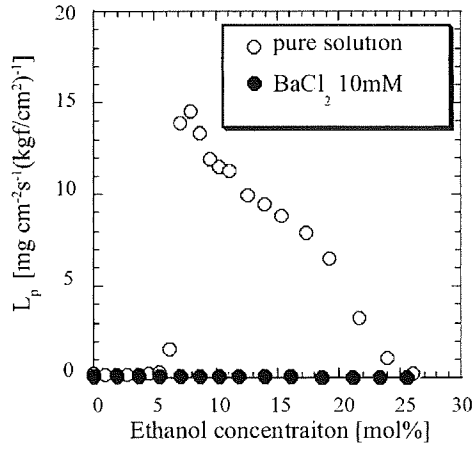

Fig. 5. Dependence on ethanol concentration of the permeability coefficient, L_p, of aqueous ethanol solution containing no ion or 10 mM $BaCl_2$ through a molecular recognition ion gating membrane at 24 °C.

A mechanism for the reentrant phase transition of poly-NIPAM [16,18] and volume phase transition of poly-NIPAM gel [17,19] has been suggested in some previous research, but it is not clear even now. We speculate that formation of a complex between the crown ether ring of BCAm and Ba^{2+} decreased the cooperativity of the phase transition along the NIPAM chain. Therefore, the size of the globule-state region became smaller and the two coil-state regions connected to each other.

3.3. Reentrant phase transition behavior of the pressure-driven flux through the molecular recognition ion gating membrane

Fig. 5 shows the pressure-driven flux of pure water and 10 mM $BaCl_2$ at 24 °C when the ethanol concentration was varied between 0 and 25 mol%. In the case of pure water, the pores of the membrane opened at around 7 mol% of ethanol, and then the flux gradually decreased. The pores finally closed at 25 mol% of ethanol. On the other hand, the pores of the membrane always closed at any concentration of ethanol at 24 °C in the presence of 10 mM $BaCl_2$. That is to say, the reentrant phase transition was lost because of 10 mM $BaCl_2$. This behavior agrees well with that of poly-NIPAM-co-BCAm as shown in Fig. 4, because the behavior of the membrane is basically determined by the properties of grafted poly-NIPAM-co-BCAm. At 12 mol% of ethanol in Fig. 4, the LCST was below 24 °C, but the phase transition gradually occurred, as shown in Fig. 3, and the copolymer shrank a little; thus, the pores were closed even at this ethanol mole ratio.

3.4. LCST/LCST-type reentrant phase transition of the pressure-driven flux through the gating membrane without the ion signal

The operating temperature was also varied between 13 and 50 °C, as shown in Fig. 6. The LCST shifted to lower temperature with increasing ethanol mole ratio. Note that the LCSTs were defined at the onset temperature of the permeation flux in the permeation experiments of this study. At the same time, the maximum pressure-driven flux through the membrane decreased and finally became zero, where the pores always closed at any concentration of ethanol because of the swelling of the grafted poly-NIPAM-co-BCAm, a behavior that coincided with the reentrant phase transition of poly-NIPAM-co-BCAm.

One unique point of poly-NIPAM-co-BCAm was also clarified from Fig. 6 during the reentrant phase transition of poly-NIPAM-co-BCAm. As previously reported [20], poly-NIPAM showed an

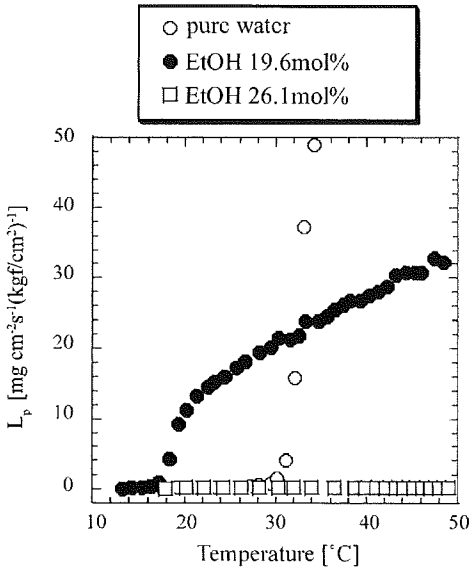

Fig. 6. Temperature dependence of the permeability coefficient of aqueous ethanol solutions through a molecular recognition ion gating membrane. Ethanol concentrations were 0, 19.6 and 26.1 mol%.

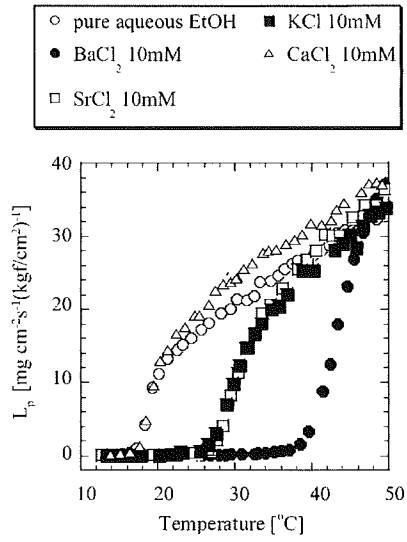

Fig. 7. Temperature dependence of the permeability coefficient of aqueous ethanol solutions containing different ion species through a molecular recognition ion gating membrane. Concentrations of ethanol and ion were 19.6 mol% and 10 mM in all cases, respectively.

LCST/UCST-type reentrant phase transition in the mixed solvent of ethanol and water. On the other hand, poly-NIPAM-co-BCAm showed an $LCST_1/LCST_2$-type reentrant phase transition, because the membrane showed an LCST at 17 °C at 19.6 mol% of ethanol (Fig. 6). Introduction of BCAm apparently affected the globule-to-coil transition of poly-NIPAM at the UCST. In the same previous research, methanol and acetone showed only an $LCST_1/LCST_2$-type reentrant phase transition, while ethanol, 1-propanol, 2-propanol, DMF and DMSO showed LCST/UCST-type reentrant phase transitions. In the LCST/UCST systems, the hydrophobic interaction was focused at the UCST because alcohols that have a UCST are more hydrophobic than methanol [20], and it is speculated that alcohols interact with poly-NIPAM by hydrophobic interactions. We speculate that the introduction of the hydrophilic crown ether ring of BCAm may contribute to weakening this hydrophobic interaction, and ethanol may behave like methanol in the case of poly-NIPAM-co-BCAm.

3.5. The effect of ion species and concentration on LCST shifts of the gating membrane

Crown ether receptors contained in the membrane recognize different ion species, which leads to a membrane response to a specific ion signal. Fig. 7 shows the temperature dependence of the pressure-driven flux in the presence of various ions such as Ba^{2+}, Sr^{2+}, Ca^{2+} and K^+ in the mixed solvent of water and ethanol in which the ethanol concentration was 19.6 mol%. The order of the width of LCST shift was $Ba^{2+} > Sr^{2+} = K^+ > Ca^{2+}$ = no ion. Compared with our previous results in aqueous solution, some points were different. First, the shift width of the LCST in the case of Sr^{2+} was larger than that in the case of K^+ in aqueous solution [1], while they showed almost the same value in the mixed solvent of water and ethanol. Second, 100 mM aqueous solutions were used in the previous study, while 10 mM solutions were used in the mixed solvent of water and ethanol. However, the LCSTs shifted almost by the same amount for each ion.

Fig. 8 shows the temperature dependence of the pressure-driven flux at different concentrations of $BaCl_2$ in the mixed solvent of water and ethanol, in which the ethanol concentration was 19.6 mol%. The LCST shifted to higher temperature with increasing concentration of $BaCl_2$. On the other hand, the pores always closed because of the swelling of the grafted copolymer when the ethanol concentration was 26.1 mol%, as shown in Fig. 9. Captured ions by the crown ether receptors do not affect the flux.

3.6. Sensitivity enhancement of the gating membrane in an aqueous ethanol solution

The LCST shift width in the presence of recognition ions was different between water and aqueous ethanol solutions, as shown in Fig. 10. In the case of an aqueous solution, the LCST shift between pure water and 100 mM $BaCl_2$ was almost 20 °C, while the LCST shift between pure solvent and 30 mM $BaCl_2$ was greater than 30 °C in the case of an aqueous ethanol solution of 19.6 mol%.

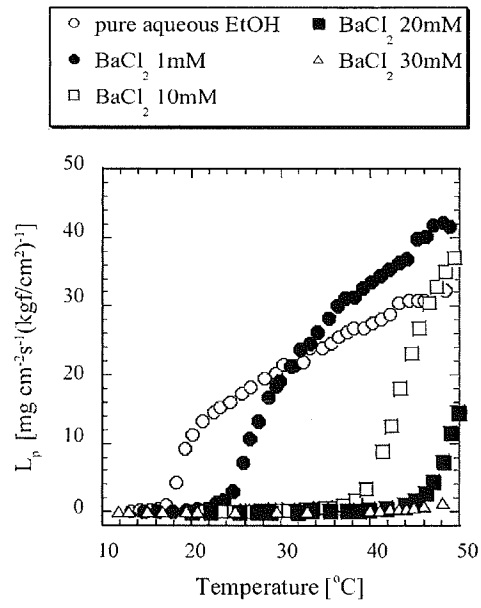

Fig. 8. Temperature dependence of the permeability coefficient of aqueous ethanol solutions containing $BaCl_2$ of different concentrations through a molecular recognition ion gating membrane. Concentration of ethanol was 19.6 mol% in all cases.